

METROLOGY AND ANALYSIS OF NANO-PARTICULATE BARIUM TITANATE  
DIELECTRIC MATERIAL

by

MATT ALLISON

B.S., Kansas State University, 2005

A REPORT

submitted in partial fulfillment of the requirements for the degree

MASTER OF SCIENCE

Department of Electrical and Computer Engineering  
College of Engineering

KANSAS STATE UNIVERSITY  
Manhattan, Kansas

2007

Approved by:

Major Professor  
Dr. Andrew Rys

## **Abstract**

Since its discovery in the 1940's, barium titanate has become one of the more popular dielectric materials for use in discrete capacitors due to its high relative permittivity. Recently, consumer electronics have decreased in size, driving the need for smaller electronic components. To fill this need, researchers have created polycrystalline barium titanate with individual grains in the nanometer scale. With this decrease in size, many problems arise. This paper will outline the effects on the dielectric properties due to shrinking the individual grains, as well as discuss techniques for measurement of this material.

# Table of Contents

Table of Contents .....	iii
List of Figures .....	v
List of Tables .....	vii
Acknowledgements .....	viii
Dedication .....	ix
1.0 Introduction .....	1
1.1 High Relative Permittivity .....	1
1.2 Capacitor Architecture .....	1
1.3 Problems Encountered .....	2
1.4 Purpose .....	2
2.0 Capacitance .....	3
2.1 Parallel Plate Representation .....	4
2.2 Dielectric Material .....	5
2.3 Real World Representation of a Capacitor .....	7
2.4 Other Capacitor Construction Methods .....	9
2.4.1 Electrolytic .....	9
2.4.2 Multi-Layer Ceramic Capacitors .....	10
3.0 Materials used in Capacitors .....	12
3.1 Other Materials .....	12
3.2 Ferroelectric materials .....	14
3.2.1 Barium Titanate .....	15
4.0 Size Effects on Dielectric Properties .....	20
4.1 Powder Size Effect .....	20
4.1.1 Historical overview .....	20
4.2 Grain Size Effect .....	23
4.2.1 A Historical Overview .....	23
4.3 Dielectric Constant .....	33
4.3.1 Internal Stresses .....	33
4.3.2 Ferroelectric Domains .....	34

4.3.3	Crystal Structure .....	34
4.3.4	Temperature .....	35
4.4	Frequency.....	35
5.0	Measurement.....	38
5.1	Measurement of the Crystal Structure .....	38
5.1.1	Crystal Structure Measurement by XRD .....	38
5.2	Measurement of Grain Size / Powder Size .....	40
5.2.1	Measurement of Size by XRD .....	41
5.2.2	Measurement of Size by SEM .....	43
5.3	Dielectric Measurement.....	44
5.3.1	Pellet Construction.....	45
5.3.2	Measuring Dielectric Constant .....	47
LCR Meter .....	47	
Raman Spectroscopy.....	49	
5.3.3	Measurement of Temperature Dependence .....	50
5.3.4	DC Resistance.....	51
5.3.5	Dielectric Strength .....	51
5.3.6	Industry Testing .....	52
6.0	Measurement Results .....	53
7.0	Conclusion and Future Work .....	57
7.1	Future Work .....	59
7.1.1	Pellet production .....	59
7.1.2	Characterization .....	59
7.1.3	Scale powder production.....	60
8.0	References.....	61

## List of Figures

Figure 2.1 Two conducting surfaces with electrical potential applied exhibit capacitance [Source Demarest].....	3
Figure 2.2 Parallel plate capacitor with no dielectric [Source Demarest] .....	5
Figure 2.3 Nonpolar dielectric structure polarizing with external potential applied .....	6
Figure 2.4 Circuit representation of a low frequency capacitance model describing parasitic losses [Source HP4284 Reference Manual].....	8
Figure 2.5 Construction of a multi-layer ceramic capacitor [Source Epcos].....	10
Figure 3.1 Bulk crystal structure for barium titanate with each ion labeled [Source Yoon] .....	15
Figure 3.2 Unit cell of barium titanate viewed from the a axis showing the polarization of titanium and oxygen ions [From Yoon].....	16
Figure 3.3 Unit cell of barium titanate viewed along a axis showing dimensionality [From Yoon] .....	16
Figure 3.4 Depiction of three crystal structures seen by barium titanate.....	19
Figure 4.1 Lattice constants with decreasing grain sizes [From Ohno et al.].....	22
Figure 4.2 Decreasing Curie temperature with decreasing powder size showing critical size of 20 nm [From Ohno et al.] .....	22
Figure 4.3 Dielectric constant increases with decreasing powder size showing critical size [From Ohno et al.].....	23
Figure 4.4 Average width of 90 degree domains at various grain sizes [Source Arlt et al.] .....	26
Figure 4.5 Dielectric constant as a function of temperature for 3 different grain sizes [From Arlt et al.] .....	27
Figure 4.6 Dielectric constant at various grain sizes [Source Arlt et al.] .....	27
Figure 4.7 Ratio of tetragonal lattice constants at decreasing grain sizes [Source Arlt et al.] .....	29
Figure 4.8 Plot showing the correlation between dielectric constant data found by Arlt et al. and Shaikh et al. [Source Arlt et al. and Shaikh et al.].....	30
Figure 4.9 Compilation of various author's findings of dielectric constant at various grain sizes [From Akdogan].....	32

Figure 4.10 Formation of 90 degree domains due to internal stresses [From Batllo et al.].....	34
Figure 4.11 Dielectric constant of 3 different grain sizes as frequency is increased [Source McNeal et al.].....	36
Figure 4.12 Dissipation factor of 3 different grain size materials as frequency is increased [Source McNeal et al.] .....	37
Figure 5.1 Example of x-ray diffraction where in a) the angle of rotation yields a destructive interference pattern, but in b) the angle yields a constructive interference pattern. Figure c) shows the measurement of the Bragg angle [From Smith and Hashemi].....	39
Figure 5.2 Sample XRD plot showing diffraction peaks at 44.9 and 45.4 degrees (2 $\theta$ ) [Source Nanoscale].....	40
Figure 5.3 Example XRD plot showing the full width half maximum measurement beta for use in grain size analysis [From Nanoscale] .....	42
Figure 5.4 SEM images of barium titanate powder produced by 3 different methods [From Yoon et al.] .....	44
Figure 5.5 Sample Raman spectra plot for single crystal barium titanate [From Ohno et al.] .....	50
Figure 6.1 XRD plot of sample from Nanoscale measured from 0 to 90 degrees .....	53
Figure 6.2 Sample XRD plot from 44 degrees to 46 degrees showing tetragonality in <200> and <002> planes [From Nanoscale].....	54
Figure 6.3 Measured dielectric constant for various reaction conditions [Source Nanoscale Corp.] .....	55
Figure 6.4 Measured dissipation factors for various reaction conditions [Source Nanoscale Corp.] .....	56
Figure 7.1 Volumetric efficiency per with variation in grain size [From Leonard et al.] .....	58

## List of Tables

Table 3.1 Dielectric constants of various materials .....	13
Table 4.1 Phase transition temperature and dielectric constant for various grain sizes [Source Leonard, Zhong] .....	31
Table 5.1 Sintering conditions and resulting grain size and porosity as reported by various authors [Source: authors listed] .....	46

## **Acknowledgements**

I would like to thank my major professor Dr. Rys for his constant encouragement. Without his help and attitude, this project would have been much more difficult.

I would also like to thank everybody at Nanoscale Corporation who had a hand in this project. Megan Winter, Justin Millette and David Jones provided nothing but help.



## **Dedication**

To my family. Without your support, none of this would have been possible.

## 1.0 Introduction

It's hard to not notice that modern consumer electronics are shrinking at a rapid rate. For this shrinking to occur, all the components inside the device must shrink as well. For most components this poses a problem, but for capacitors, whose capacitance value depends directly on its physical size, it poses a major problem. To combat this problem, manufacturers have taken two approaches; 1) introduce dielectric materials with high relative permittivity to boost the capacitance, 2) create a new capacitor architecture that will not only decrease physical size, but also increase the total capacitance of the device.

### 1.1 High Relative Permittivity

With relative permittivity, also known as the dielectric constant, in the numerator of the parallel plate capacitance equation, capacitance is directly proportional to the relative permittivity. While previous dielectric materials have relative permittivities less than 10, polycrystalline barium titanate has shown a relative permittivity between 1000 and upwards of 6000 [1]. With a dielectric constant this high, the area of the plates in the capacitor can be hundreds of times less.

### 1.2 Capacitor Architecture

The typical architecture of a capacitor is two parallel plates separated by a specific distance that is filled with a dielectric material. Multi-layer ceramic capacitors (MLCC's) take this architecture and stack hundreds of layers on top of each other in a very small package, thereby creating hundreds of parallel capacitors. Since capacitors in parallel add, this

architecture multiplies the total area of each layer by the number of total layers, creating a large capacitor in a small package.

### 1.3 Problems Encountered

In modern production techniques, both of these approaches are employed, using barium titanate dielectric material in MLCC's. Since the conductor layers internal to a MLCC are separated by a dielectric on the order of 2 or 3 microns in thickness, the polycrystalline barium titanate must be formed with powder crystallites much smaller than this. Typical powders have individual crystallites in the nanometer range. This reduction in size comes with a share of problems including

- Reduction of dielectric constant
- Shift of Curie temperature
- Phase transitions of crystal structure
- Loss of ferroelectric domains

Each of these issues will be discussed in subsequent chapters.

### 1.4 Purpose

The purpose of this report is to provide a discussion of various problems encountered with a reduction in size of individual crystallites of barium titanate as well as measurement techniques for characterizing the created dielectric material. This report will aid researchers in dielectric measurement of produced barium titanate powder and understanding of the measurement results. Through the reading, certain critical measurements will be presented for optimization of the barium titanate production process.

## 2.0 Capacitance

In order to understand the characteristics of a dielectric material, it is imperative to understand the concept of capacitance, since this concept is employed to measure and characterize the dielectric material. The concept of capacitance is one taught in elementary circuit theory courses as an energy storage device. The easiest way to visualize capacitance is through two conducting surfaces separated by a distance.

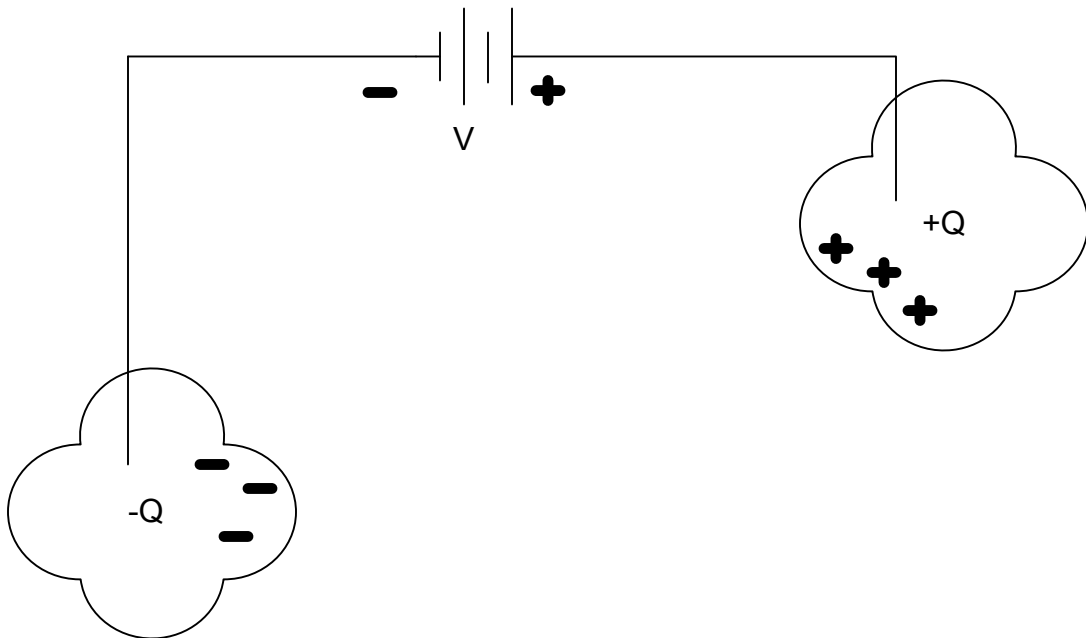


**Figure 2.1 Two conducting surfaces with electrical potential applied exhibit capacitance [Source Demarest]**

When an electrical potential is applied across the two conducting surfaces, charges will accumulate on the surfaces, positive charges on the surface with the highest potential, and an equal negative charge on the surface exposed to the most negative potential. The capacitance can then be defined as the charge accumulated per potential applied, shown in the following equation.

$$C \equiv \frac{Q}{V} \quad (2.1)$$

In this equation, Q is the charge accumulated on a surface in Coulombs, and V is the potential applied in Volts. Capacitance can then be found in Coulombs per Volt, or Farads. A Farad is a very large unit, so capacitance values are often expressed in fractions of this amount, typically picofarads (pF) or microfarads (uF) [2].

## 2.1 Parallel Plate Representation

The basic and most widely used form of capacitor is the parallel plate capacitor. In this form, the two conducting surfaces of the previous example are large two dimensional sheets of conductive material. If these sheets are of area A, and separated by a distance D in a vacuum, the capacitance of the system can be described by the following equation.

$$C = \epsilon_0 \frac{A}{D} \quad (2.2)$$

where  $\epsilon_0$  is the permittivity of free space ( $8.85 \times 10^{-12}$  F/m). This equation shows a direct relationship between the total capacitance of the system and the area of the conductors, and an inverse relationship to the distance between the conductive plates.

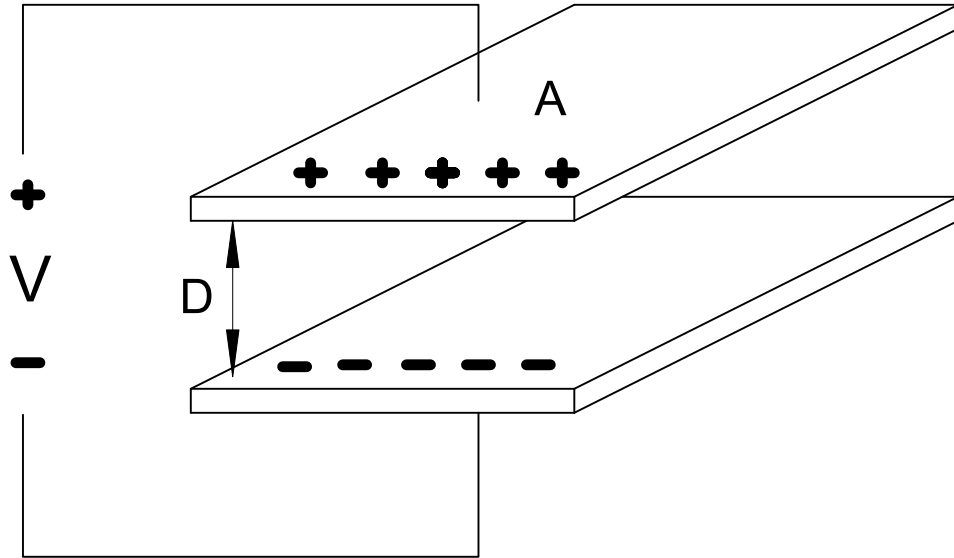


**Figure 2.2 Parallel plate capacitor with no dielectric [Source Demarest]**

In this sense if a larger capacitance value is desired, the area of the plates would need to be increased, or the distance between them decreased. Each of these options creates a problem, the first with physical size restrictions, and the second with high voltage breakdown (to be explained later). A third option exists to increase the capacitance value for a static size, this is to insert a dielectric material in between the plates.

$$C = \epsilon_0 \epsilon_r \frac{A}{D} \quad (2.3)$$

In this equation,  $\epsilon_r$  is the relative permittivity of the dielectric material. The relative permittivity is also quoted as the dielectric constant ( $k$ ), in this paper the two terms will be used interchangeably.

## 2.2 Dielectric Material

Dielectric materials are characterized by charges tightly bound to the individual nuclei, in contrast to a conductor which has charges which are free to move about inside the atomic structure. In polar dielectrics, a shift has occurred in the atomic structure such that the positive

and negative charges have an asymmetrical alignment producing an electric dipole. Nonpolar dielectric materials lack this inherent dipole in the absence of a polarizing field, however when an external potential is applied, a dipole forms from a shift in the electron cloud [2].

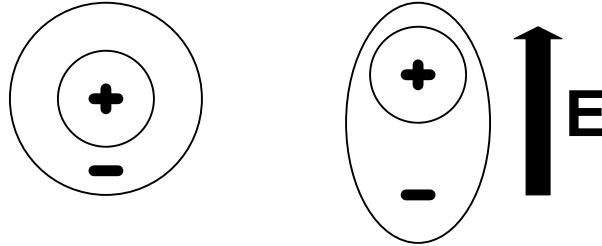


**Figure 2.3 Nonpolar dielectric structure polarizing with external potential applied**

This polarization results in a dipole moment ( $\mathbf{p}_k$ ) of each polarized atomic structure. Though these are discrete points, from a macroscopic view they tend toward a continuous distribution ( $\mathbf{p}$ ).

$$\mathbf{P} = \lim_{\Delta v \rightarrow 0} \frac{\sum_{k=1}^{N\Delta v} \mathbf{p}_k}{\Delta v} \quad (2.4)$$

In simple, homogenous, dielectric media,  $\mathbf{P}$  is always proportional to  $\mathbf{E}$ ; thus

$$\mathbf{P} = \epsilon_0 \chi_e \mathbf{E} \quad (2.5)$$

In this equation,  $\chi_e$  is the electric susceptibility, a unitless constant that describes the dielectric's ability to form dipoles. In anisotropic dielectric material, the susceptibility is described by a tensor of three dimensions [2]. Due to the added complexity of anisotropic dielectric material, all dielectrics for this discussion will be assumed isotropic.

The electric flux density can be found

$$\mathbf{D} = \epsilon_0 \mathbf{E} + \mathbf{P} \quad (2.6)$$

Substituting equation 2.5,

$$\mathbf{D} = \varepsilon_0 (\chi_e + 1) \mathbf{E} \quad (2.7)$$

$$\mathbf{D} = \varepsilon \mathbf{E} \quad (2.8)$$

$$\varepsilon = \varepsilon_0 \varepsilon_r \quad (2.9)$$

$$\varepsilon_r = (1 + \chi_e) \quad (2.10)$$

With this,  $\varepsilon_r$  is defined as the relative permittivity.

Permittivity can also be described as a complex sum of a real permittivity, seen by the capacitance and an imaginary permittivity describing the (generally unwanted) absorption of energy by the medium. The imaginary permittivity describes a loss due to polarization and other factors.

$$\hat{\varepsilon} = \varepsilon' + \varepsilon'' \quad (2.11)$$

In this equation,  $\varepsilon'$  describes the real part of the permittivity, and  $\varepsilon''$  describes the imaginary part. The loss tangent can be found by the following equation.

$$\tan(\delta) = \frac{\varepsilon''}{\varepsilon'} \quad (2.12)$$

This metric describes the proportion of imaginary permittivity to real permittivity, or the relationship between energy absorption and energy storage in the dielectric material. Complex permittivity is somewhat obscure to conceptualize; a circuit model is used to describe the parasitic effects of the imaginary permittivity.

### 2.3 Real World Representation of a Capacitor



Ideally the capacitor is a purely capacitive element, with no parasitic losses, however, in the real world this is much different. A real world model of a capacitor was developed to include dielectric losses and other factors not seen in the ideal parallel plate assumption.

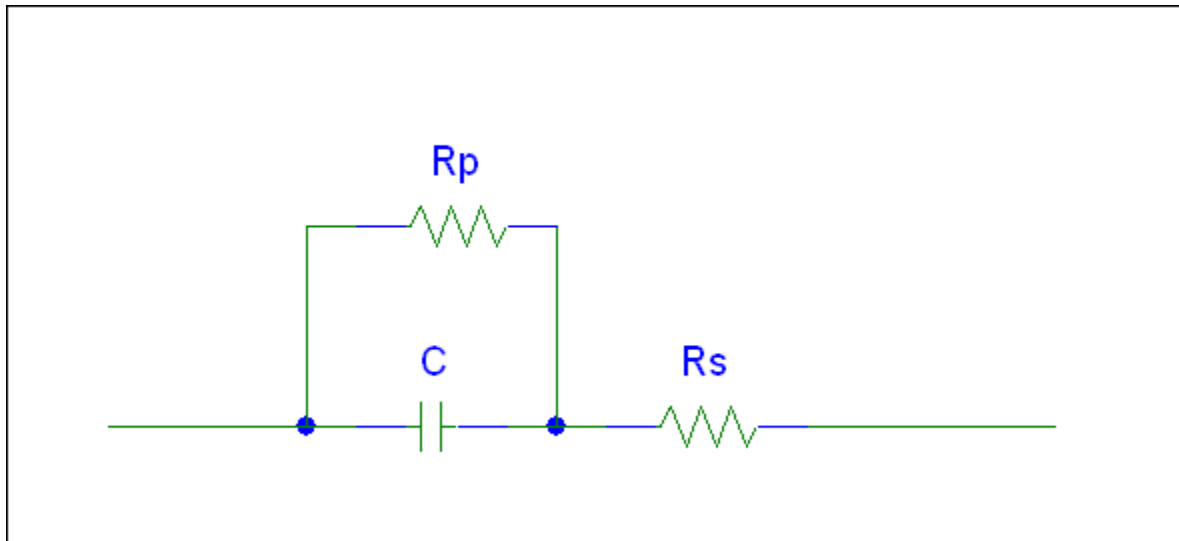


**Figure 2.4 Circuit representation of a low frequency capacitance model describing parasitic losses [Source HP4284 Reference Manual]**

This is a simple low frequency model of a capacitor describing the parasitic effects of the complex permittivity and physical construction. The parallel resistance models the polarization losses due to hysteresis and relaxation of the dipoles, while the series resistance models losses due to the physical construction of the capacitor including lead resistance, and non-ideal connections between components. When the capacitance is small, the parallel resistance has more of an effect on the system, and the series resistance can be neglected [3]. This is the model used for measurement devices described in a later section.

## 2.4 Other Capacitor Construction Methods

The quintessential construction method used in most production capacitors is the parallel plate method described earlier. This is an easy production method employed in discrete ceramic disc capacitors. This is not the only method of constructing discrete capacitors, this section will describe some of the more popular alternative capacitor construction methods.

### 2.4.1 Electrolytic

One way of making a large capacitance is to use large sheets of aluminum foil stacked on top of each other, increasing the area of the conductors. These sheets can then be covered with a thin dielectric layer and rolled to decrease the package size. This is essentially how electrolytic capacitors are made. The dielectric layer is composed of a very thin layer of aluminum oxide that is grown on the foil. It is necessary to place the second conducting plate as close to this aluminum oxide as possible to eliminate any voids or cavities, so a conducting liquid, or electrolyte, is used in place of a second aluminum plate. To avoid sloshing liquid inside a production capacitor, this liquid is replaced with electrolytic soaked paper [4].

The oxide is deposited on the aluminum foil through an electrolytic process, where the foil is submerged in a liquid and a current is passed through, depositing aluminum oxide on the surface of the foil. The deposition method is very similar to the final construction of the capacitor, making it essentially self healing in the sense leakage current inside the capacitor will rebuild the dielectric layer where voids are present. The process is reversible though, making the finished capacitor polar. If the polarity is reversed, the oxide layer is destroyed resulting in leakage current, which will break down the oxide layer further, until total destruction of the capacitor occurs [4].

## 2.4.2 Multi-Layer Ceramic Capacitors

With a decrease in size of discrete components, the overall size of capacitors followed suit. However with the physical size of the capacitor playing a huge role in the capacitance value, this was difficult. A solution was found in the form of stacking many layers of dielectrics on top of alternating conductors, in effect forming hundreds of small capacitors in parallel [5]. From the previous equation for capacitance of parallel plates (Equation 2.3), the capacitance of a multi-layer ceramic capacitor (MLCC) can be found [6].

$$C = \epsilon_r \epsilon_0 \frac{(n-1)A}{d} \quad (2.13)$$

The capacitance is increased by a factor of (n-1) where n is the number of layers in the capacitor.

Until 1995, the internal electrodes of most MLCCs were comprised of expensive noble metals such as alloys of silver and palladium. These have been replaced by base metals such as nickel or copper and in effect the price has reduced considerably [5]. Shown below is a model of the construction of a MLCC. The connection of internal conductors to opposing sides creates the parallel capacitances.

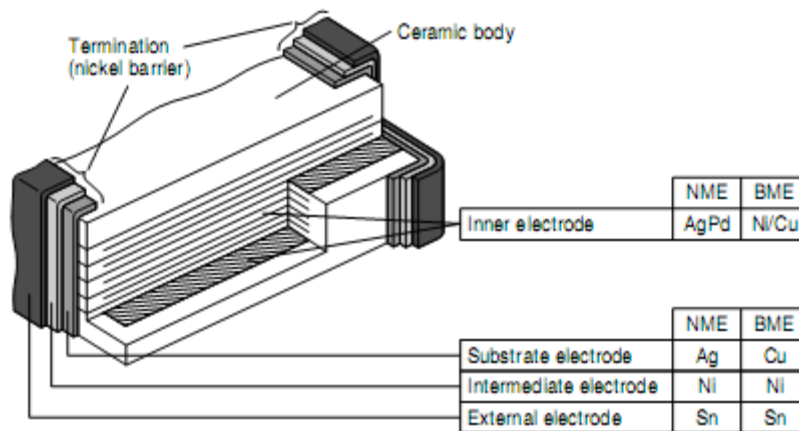


Figure 2.5 Construction of a multi-layer ceramic capacitor [Source Epcos]

The MLCC production process is started with a mixture of ceramic powder and binder and then formed into a green ceramic sheet by tape casting. The internal electrode plates are then screen printed on the sheets and stacked to the desired number of layers. This stack is then laminated and cut to size and heated to remove the binder and then sintered [5].

Layers of two to three microns in thickness stacked in several hundred layers tend to yield the highest volumetric efficiency. A poor end product results if air pockets or pores of poor ceramic dispersion are created in even one of these layers. Each sintered layer is desired to contain 5 grains in thickness for overall long-term stability in terms of a final capacitor product. With this in mind, ceramic powders of spherical sub-micron grains which are chemically homogenous and unagglomerated are desired for production [5].

### **3.0 Materials used in Capacitors**

Many materials are used for dielectrics in discrete capacitors. Different materials provide different characteristics, some have higher breakdown voltages, and some have higher capacitance per volume. The end user can choose the desired capacitor based upon these individual characteristics.

#### **3.1 Other Materials**

This section will provide a simple overview of various materials and their dielectric constants. Table 3.1 shows some of these materials. Most of the materials provided in this table are not typical dielectric materials, but are provided for comparison of dielectric constant among everyday materials and the reported dielectric constant for barium titanate later.

Materials from this table typically used in standard capacitors include paper, air, and mylar. Each of these has a dielectric constant below 5, resulting in large capacitors for a given capacitance value. This has led to research in new materials with very high dielectric constants.

**Table 3.1 Dielectric constants of various materials**

<b>Material</b>	<b>Min</b>	<b>Max</b>	<b>Material</b>	<b>Min</b>	<b>Max</b>
Air	1	1	Nylon	3.4	22.4
Amber	2.6	2.7	Paper	1.5	3
Asbestos fiber	3.1	4.8	Plexiglass	2.6	3.5
Bakelite	5	22	Polycarbonate	2.9	3.2
Beeswax	2.4	2.8	Polyethylene	2.5	2.5
Cambric	4	4	Polyimide	3.4	3.5
Carbon Tetrachloride	2.17	2.17	Polystyrene	2.4	3
Celluloid	4	4	Porcelain	5	6.5
Cellulose Acetate	2.9	4.5	Quartz	5	5
Durite	4.7	5.1	Rubber	2	4
Ebonite	2.7	2.7	Ruby Mica	5.4	5.4
Epoxy Resin	3.4	3.7	Selenium	6	6
Ethyl Alcohol	6.5	25	Shellac	2.9	3.9
Fiber	5	5	Silicone	3.2	4.7
Formica	3.6	6	Slate	7	7
Glass	3.8	14.5	Soil dry	2.4	2.9
Glass Pyrex	4.6	5	Steatite	5.2	6.3
Gutta Percha	2.4	2.6	Styrofoam	1.03	1.03
Isolantite	6.1	6.1	Teflon	2.1	2.1
Kevlar	3.5	4.5	Titanium Dioxide	100	100
Lucite	2.5	2.5	Vaseline	2.16	2.16
Mica	4	9	Vinylite	2.7	7.5
Micarta	3.2	5.5	Water distilled	34	78
Mylar	3.9	3.9	Waxes, Mineral	2.2	2.3
Neoprene	4	6.7	Wood dry	1.4	2.9

### 3.2 Ferroelectric materials

The term ferroelectricity is a misnomer used at the time of its discovery in the 1920's to describe a phenomena analogous to the ferromagnetic phenomena of iron. Ferroelectric materials do not show any connection with iron (in Latin: ferrum) at all. The term was devised to explain a spontaneous polarization upon cooling below a Curie temperature as well as a display of ferroelectric domains and a ferroelectric hysteresis loop. Since the discovery of ferroelectric characteristics materials that exhibit ferroelectric qualities have been widely studied and employed in practical applications [7].

Ferroelectric ceramics can find a use in applications across a wide range of topics, but are primarily focused in a few key areas.

- Dielectrics with high relative permittivity, low dissipation, and high frequency response. These materials have already found a niche in dielectrics for Multi-Layer Ceramic Capacitors (MLCCs). Ferroelectric materials have been used as high k insulator layers for DRAM cells where high charge storage density is desired [1]. Applications of embedded capacitive polymers in printed circuit boards [8] are on the horizon.
- Transducers and sensors that employ piezoelectric characteristics. Electrical to mechanical energy conversion relies on the piezocharge coefficient, whereas the mechanical to electrical energy conversion uses the piezovoltage coefficient of the material [1].
- Positive temperature coefficient of resistance applications. The positive temperature coefficient of a specific ferroelectric material ( $\text{BaTiO}_3$ ) makes it suitable for use in a construction where the polarization can control the charge across a Schottky barrier [1].

In the category of high k dielectrics, ferroelectric materials including some form of barium titanate have been marveled for the past half of a century. The focus of this paper will be in the high dielectric constant of the material for use in discrete capacitors. The category of

ferroelectric materials for use as high dielectric constant materials is not limited to barium titanate. Research is proceeding on ferroelectrics such as lead zirconate titanate and lead magnesium niobate, the latter has shown a dielectric constant upwards of 20,000, but shows a large polarization hysteresis [7].

### 3.2.1 Barium Titanate

Barium titanate is a perovskite with the chemical notation  $\text{BaTiO}_3$ . Perovskites are crystals with a structure  $\text{ABO}_3$  where A and B are cations of different sizes. The unit cell is of a tetragonal formation shown in Figure 3.1.

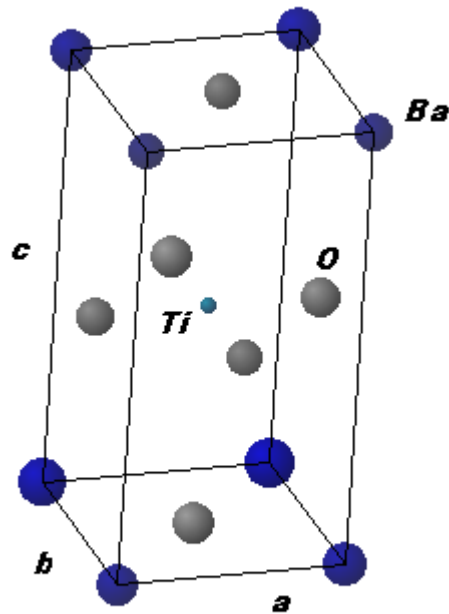


**Figure 3.1 Bulk crystal structure for barium titanate with each ion labeled [Source Yoon]**

This crystal structure for bulk barium titanate has the titanium cation in the middle with oxygen at the faces of each side and barium ions at the corners. The titanium ion is not exactly



in the center of the structure, but shifted upwards along the  $c$  axis giving the unit cell a polarization [5]. This is shown in Figure 3.2.

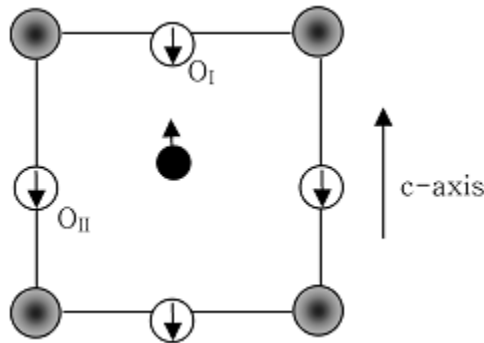


**Figure 3.2 Unit cell of barium titanate viewed from the  $a$  axis showing the polarization of titanium and oxygen ions [From Yoon]**

The dimensions of the bulk crystal structure are shown for the titanium and oxygen ions in Figure 3.3.

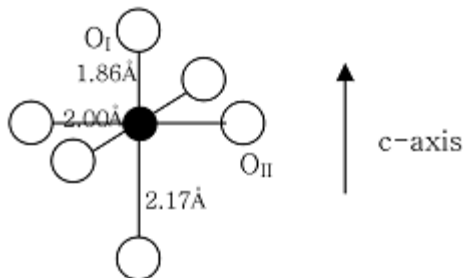


**Figure 3.3 Unit cell of barium titanate viewed along  $a$  axis showing dimensionality [From Yoon]**

Barium titanate's high relative permittivity characteristics were found in 1943 in several different parts of the world independently [1]. Since that time barium titanate has become one of the most researched dielectric materials and one of the most widely used for small discrete components. The dielectric constant of bulk material depends on the orientation. Along the  $a$  axis the dielectric constant is around 4000, but along the  $c$  axis it is only around 200. In the 1950's the dielectric property was found to increase for material ground into fine grains and

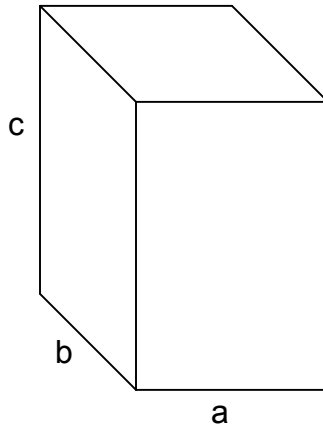
sintered into a ceramic. This polycrystalline material is no longer dependent on orientation since many crystal orientations exist internal to the polycrystalline material. The dielectric constant is now an average between that of the  $a$  axis and that of the  $c$  axis. As the powder was ground to finer and finer sizes, the dielectric constant was found to increase to a critical point and then decrease at sizes smaller than this critical point.

Barium titanate, like other ferroelectric materials, exhibits ferroelectric domain structures. These domains are regions of dipoles oriented similarly. When an external potential field is applied these domains align with the external field in an effort to minimize the total energy of the system. Many authors have attributed the increase in dielectric constant with grain sizes less than a micron to the increase in domain wall density, and residual stresses [9]. These residual stresses are relieved by formation of  $90^\circ$  domain walls with a believed lower width limit of around  $1\mu\text{m}$ . Grain sizes less than this critical  $1\mu\text{m}$  show no  $90^\circ$  domain structure and no way of alleviating internal stresses, leading to still high relative permittivities. A further decrease in grain size destabilizes the tetragonal crystal structure and transitions into other crystal formations.

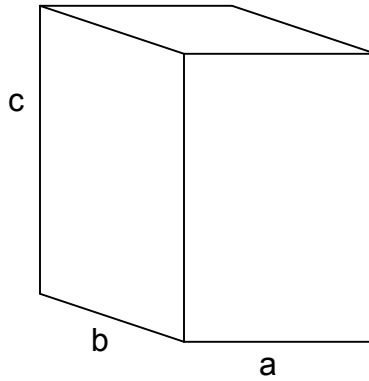
The unit cell has been found to have 5 different phases corresponding to phase transitional temperatures. At very low temperatures, the unit cell has a rhombohedral structure, and upon increase to  $-90^\circ\text{C}$  the crystal structure becomes orthorhombic. The phase transitions at  $0^\circ\text{C}$  from orthorhombic to tetragonal. The tetragonal phase extends to the Curie point at  $120^\circ\text{C}$ , after this temperature, the crystal structure is cubic and all ferroelectric tendencies have been relieved. At about  $1450^\circ\text{C}$  the crystal structure becomes hexagonal [5]. This transition is well above any operating or processing temperatures, so this phase will be neglected in this report.

The tetragonal phase, as explained earlier is an elongation of one axis from a cubic, so two axes are equal, with the third axis longer, as shown in Figure 3.4. The orthorhombic phase yields a crystal structure with no lattice axes equal, while the rhombohedral unit cell has all axes equal but none of the angles between the axes are  $90^\circ$ .

### Tetragonal $a=b \neq c$



### Orthorhombic $a \neq b \neq c$



### Rhombohedral $a=b=c$

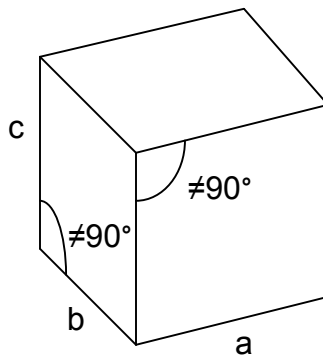


Figure 3.4 Depiction of three crystal structures seen by barium titanate

## 4.0 Size Effects on Dielectric Properties

The size of the individual powder or grain has been shown to significantly influence the dielectric properties of Barium titanate. This section will describe this size effect first in powders and then sintered ceramics. The effect is similar, but the analysis is different due to boundary conditions.

Varying terminology is used to describe the smallest granular component of the dielectric structure. For this paper, the term powder size (L) will refer to the smallest particulate in a loose powder form, while the term grain size (G) will refer to the smallest particulate in a ceramic material. In an attempt to alleviate any confusion, the term particle size will not be used, since it can be used in place of grain size or as another metric all to itself.

The measurement of the grain or powder size parameter has held many definitions. Most commonly the definition for the size of a grain or powder is the diameter of a sphere that fully encompasses the individual grain or powder [1]. The size is reported as an average of many different measurements, and not the smallest or largest present in the system.

### 4.1 Powder Size Effect

While the dielectric properties of ceramic barium titanate have been researched for over half a century, the same properties of loose powder form have just started being researched. This arises from a difficulty in extracting the intrinsic properties of barium titanate from the extrinsic measurements gathered from the composite nature of the powder mixture [10]. Due to this most of the focus will be primarily on the dielectric properties of ceramic barium titanate. This section will provide a lighter historical overview of research in barium titanate powders, most of which being in the crystal structure, which will be discussed in later sections.

#### 4.1.1 Historical overview

In 1954, Anliker et al. found the tetragonality of crystals, determined by x-ray diffraction, began to decrease in powders 5  $\mu\text{m}$  and smaller. At the same time it was noted the fine powders maintained tetragonality to temperatures well above, often several hundred degrees, that of the transitional temperature for larger crystals [1].

In 1966, Kiss et al. determined the crystal structure of powders through use of transmission electron microscopy. Powders of size 100 nm and smaller were determined to have a cubic structure and powders of size 150 nm and greater were determined to be in a tetragonal phase [1].

In 1989, Uchino et al. found the Curie temperature to decrease with decreasing powder size. This was in sharp contrast to the findings for other ferroelectric materials such as Lead-Lanthanum-Zirconate-Titanate (PLZT) which was found to have the opposite effect. Through experimental analysis, using XRD to measure grain size with Scherrer's equation, and Curie temperature by watching for abrupt changes in crystal structure, the lattice constants were plotted with changing temperature. Extrapolating the experimental data with the equation below, the authors found a critical size for barium titanate powder to be about 120nm. This critical size occurs when the powder size causes the Curie temperature to drop to room temperature [11].

$$T_C = 128 - \frac{700}{(d - 110)} \quad (4.1)$$

In 2004, Ohno et al. found a trend similar to that reported by Uchino et al.. Ohno measured the crystal's lattice constants with XRD and calculated grain size through Scherrer's equation. They found the lattice constants decrease, with a sudden convergence to a cubic structure at powder sizes less than 30 nm. This correlates with the Curie temperature dropping significantly at these powder sizes, and eventually crossing room temperature at a critical size of

20 nm. Figure 4.1 shows the lattice constants along the  $a$  and  $c$  axis decrease with a decrease in powder size.

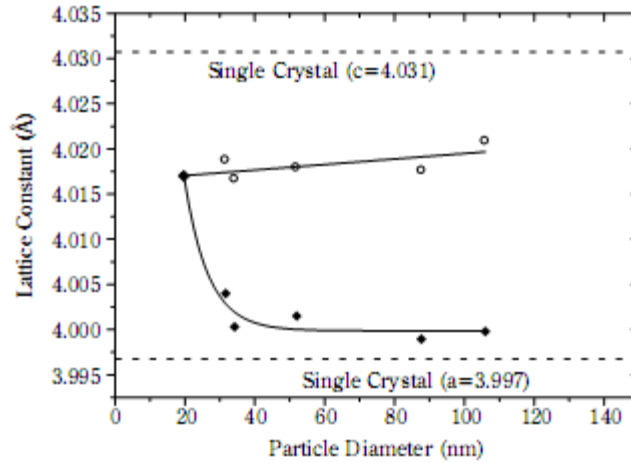


Figure 4.1 Lattice constants with decreasing grain sizes [From Ohno et al.]

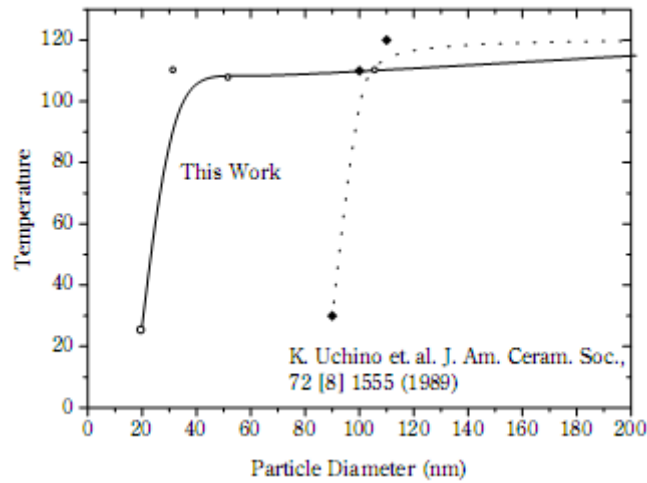


Figure 4.2 Decreasing Curie temperature with decreasing powder size showing critical size of 20 nm [From Ohno et al.]

Ohno et al. also found the room temperature dielectric constant of the powder increased at the smallest powder sizes. This observation conflicts with previous models, but correlates with the shifting of the Curie point. This marked one of the first times dielectric constant was measured for barium titanate powders, and done through use of Raman spectra analysis [10].

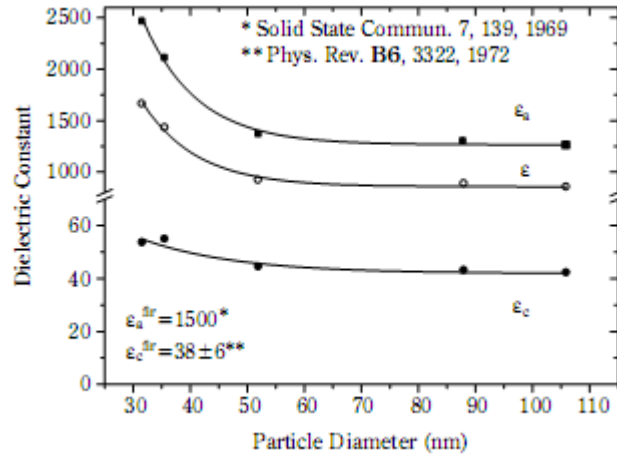


Figure 4.3 Dielectric constant increases with decreasing powder size showing critical size [From Ohno et al.]

## 4.2 Grain Size Effect

Like with the powder, the size of the grains of a sintered ceramic has a large effect on the dielectric properties.

### 4.2.1 A Historical Overview

In order to understand where the research is at this time, and why researchers are only so far, it is necessary to look at the history of research into the grain size effects of the dielectric properties of barium titanate material. The dielectric effects of grain size on crystal structure, temperature dependence, relative permittivity, and polarization domains will all be discussed in this section, among a few other topics.

The year 1950 saw Harwood et al. show one of the first works on the grain size dependence on the crystal structure. These authors found when the material was sintered below 800° C, the room temperature crystal structure showed a cubic alignment. As the sintering temperature was increased from 400° C to 800° C the volume of the cubic unit cell decreased. Sintering at temperatures above 800° C yielded a room temperature crystal structure that was



tetragonal with the tetragonality ( $c/a$ ) increasing with increased temperature [1]. The link between sintering temperature and grain size was not discussed in this report, but this link was made in later papers.

In the same decade, Kneipkamp and Heywang, in 1954, reported a dielectric constant of 3500 at room temperature for fine grained material. This was at least twice the dielectric constant of course grained material at the time. No grain size dimensionality was reported with these results. Egerton and Koonce, in 1955, reported a similar dielectric constant of 3400 at room temperature for fine grained, high purity material. These authors also found a decreased ease of domain alignment for this fine-grained material [1].

In 1962, Jonker and Noorlander tested the effects of composition ratios of the barium titanate mixture. Extra titania ( $\text{TiO}_2$ ), up to 4% was added. They noticed the mixture with 4% more titania had well defined tetragonality as a powder, but when the material was sintered into a ceramic, the tetragonality ( $c/a$ ) was reduced. When the sintered ceramic was pulverized back into powder form, the tetragonality returned to pre-sintered values [1]. These reports were later contradicted by Bradley in 1968 who found the tetragonality ratio ( $c/a$ ) was proportional to grain size only, not composition ratios.

Carmichael, in 1964, and Miller, in 1967, both found the room temperature dielectric constants to be 4000, for Miller, and 4500, for Carmichael, with grain sizes around  $1\ \mu\text{m}$ . Carmichael found increased temperature stability at this grain size. Miller decreased the size of course grained material from 60 to  $25\ \mu\text{m}$  and found a decrease in dielectric constant around the transition from tetragonal crystal structure to orthorhombic [1].

In 1976, Kinoshita and Yamaji analyzed the dielectric properties of barium titanate ceramic with average grain sizes ranging from  $15.5\ \mu\text{m}$  down to  $1.1\ \mu\text{m}$ . At room temperature

the dielectric constant of the smaller grain size was over 5000, while the largest grain size had a dielectric constant over three times smaller at just over 1500. While the ceramic was in the ferroelectric state the dielectric constant was found to be heavily dependent on the grain size. The same was not true for the paraelectric state. As the temperature was increased above the Curie point, the grain size showed little to no effect on the dielectric constant with the dielectric constant following the Curie-Weiss law very closely. In this state, the Curie constant, and Curie-Weiss temperature stay similar across all grain sizes [12].

The Curie-Weiss Law is a way of determining the electrical susceptibility of a ferroelectric material above the Curie temperature ( $T_c$ ) when the material transitions into a paraelectric form. In this form, the material loses the alignment of the dipole structure and reverts to a cubic crystal structure [13]. This mean field approximation of the susceptibility ( $\chi$ ) takes the form:

$$\chi = \frac{C_c}{T - T_c} \quad (4.2)$$

where  $C_c$  is the Curie constant. The susceptibility can then be related to the capacitance through the following equation.

$$C = C_0 (1 + \chi) \quad (4.3)$$

In this case,  $C_0$  is the capacitance without dielectric, or the capacitance in a vacuum given by the equation below.

$$C_0 = \frac{\epsilon_0 A}{d} \quad (4.4)$$

In 1985, Arlt et al. provided a report that tackled most aspects of grain sized dependence on the dielectric properties of BaTiO<sub>3</sub> at that time. The focus of the paper was on the 90° domain widths internal to the grains and how they affected various properties. When these 90° domains were measured with decreasing grain size, the plot in Figure 4.4 was achieved. The domain widths for grain sizes greater than 10 μm remained fairly constant, while between 1 μm and 10 μm the domain widths decreased in proportion to  $\sqrt{G}$ . When the plot was extrapolated, the 90° domains appeared to disappear at grain sizes of 0.4 μm [9].

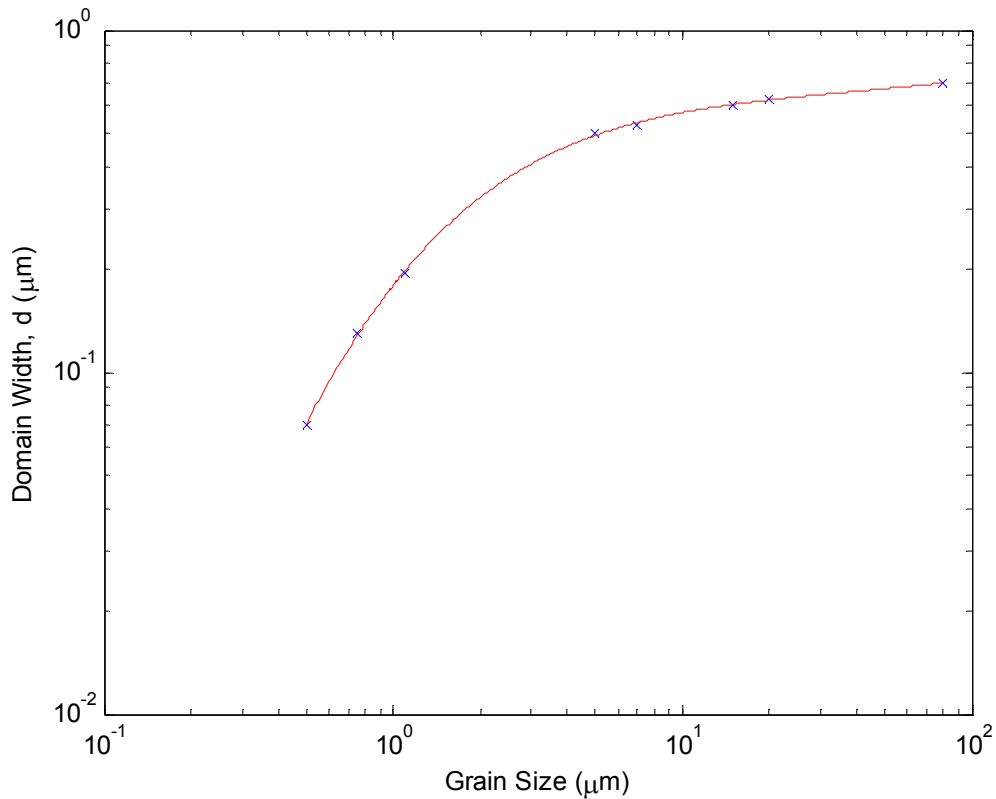


**Figure 4.4 Average width of 90 degree domains at various grain sizes [Source Arlt et al.]**

The dielectric constant was measured against temperature and presented in Figure 4.5. The highest dielectric constants in the ferroelectric state were for grain sizes between 0.7 μm and 1 μm. Further decrease in grain size down to a size of 0.28 μm decreased the dielectric constant.

Of note also is the dielectric constant's dependence on grain size in the paraelectric state at the small grain sizes tested ( $G < 0.7\mu\text{m}$ ).

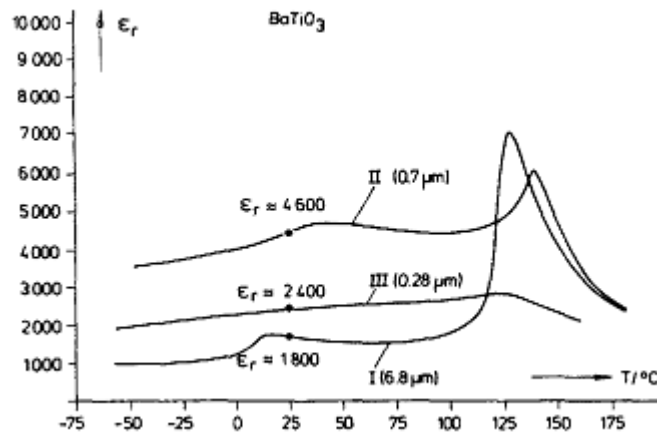


Figure 4.5 Dielectric constant as a function of temperature for 3 different grain sizes [From Arlt et al.]  
 Figure 4.6 shows the measured dielectric constant versus grain size.

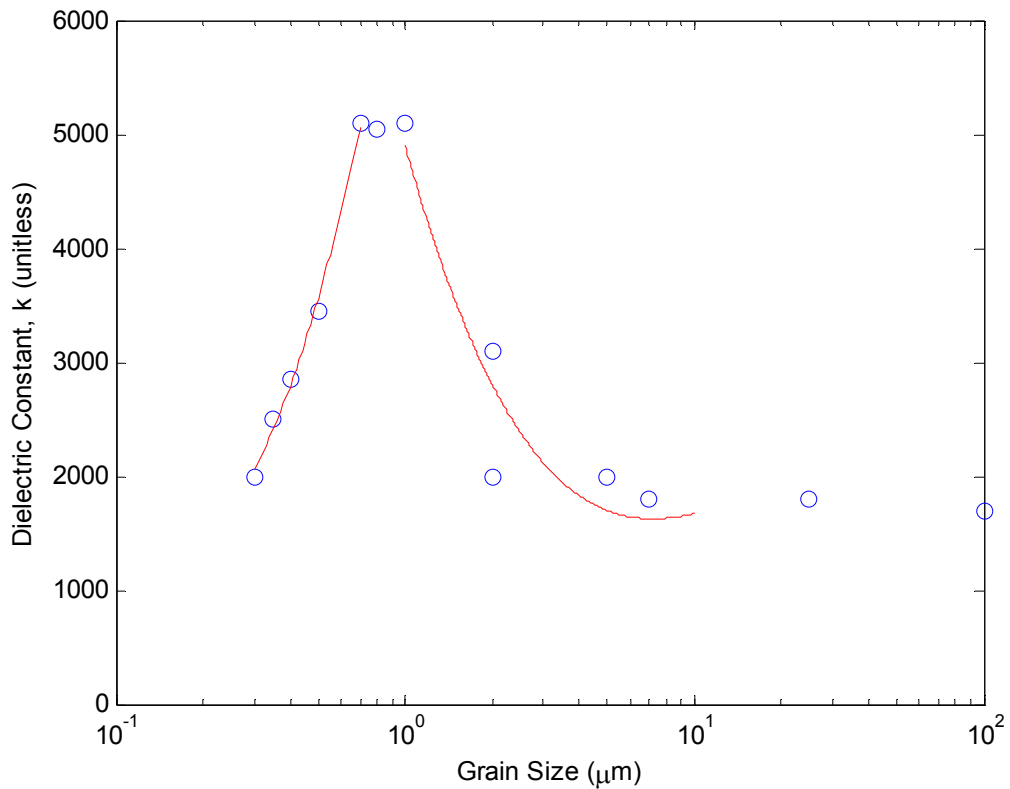


Figure 4.6 Dielectric constant at various grain sizes [Source Arlt et al.]

From their findings, Arlt et al. proposed the total dielectric constant of barium titanate ceramics could be found from the sum of the contributions of the single crystal volume and the ferroelectric domain walls moving in the electric field.

$$\varepsilon_r(T) = \varepsilon_{r,vol}(T) + \varepsilon_{r,dom}(T) \quad (4.5)$$

From this assumption, the authors posed a model to approximate the dielectric constant for grain sizes down to 1 $\mu\text{m}$ . Assuming the volumetric relative permittivity remained constant, the authors found the following.

$$\varepsilon_r = \varepsilon_{r,vol} + (kA_{tot}) \quad (4.6)$$

$$\varepsilon_r = 1000 + \frac{2200}{\sqrt{a/(\mu\text{m})}} \quad (4.7)$$

$$\varepsilon_r = 1000 + \frac{500}{D} \quad (4.8)$$

In the equations,  $A_{tot}$  refers to the total area of the 90 degree domain walls per volume.

With decreasing grain size this area will increase proportional to:  $A \sim \frac{1}{D} \sim \frac{1}{\sqrt{a}}$ .  $D$  in this case

refers to the domain width given in the previous section. The authors found the volumetric relative permittivity to be 1000.

Crystal lattice structural changes were attributed to the decrease in dielectric constant at grain sizes less than 0.7 $\mu\text{m}$ . It was noticed that at grain sizes  $G > 1.5 \mu\text{m}$  the tetragonal crystal lattice parameters ( $c/a - 1$ ) remained a constant 1.02%, however at grain sizes  $G < 1 \mu\text{m}$  the parameters distorted at room temperature ( $c/a - 1$ )  $< 1\%$  becoming more orthorhombic. At  $G = 0.28 \mu\text{m}$  grain size, the crystal structure did not resemble any known ferroelectric phases of

barium titanate, but was reported as orthorhombic [9]. Figure 4.7 shows the crystal structures for various grain sizes.

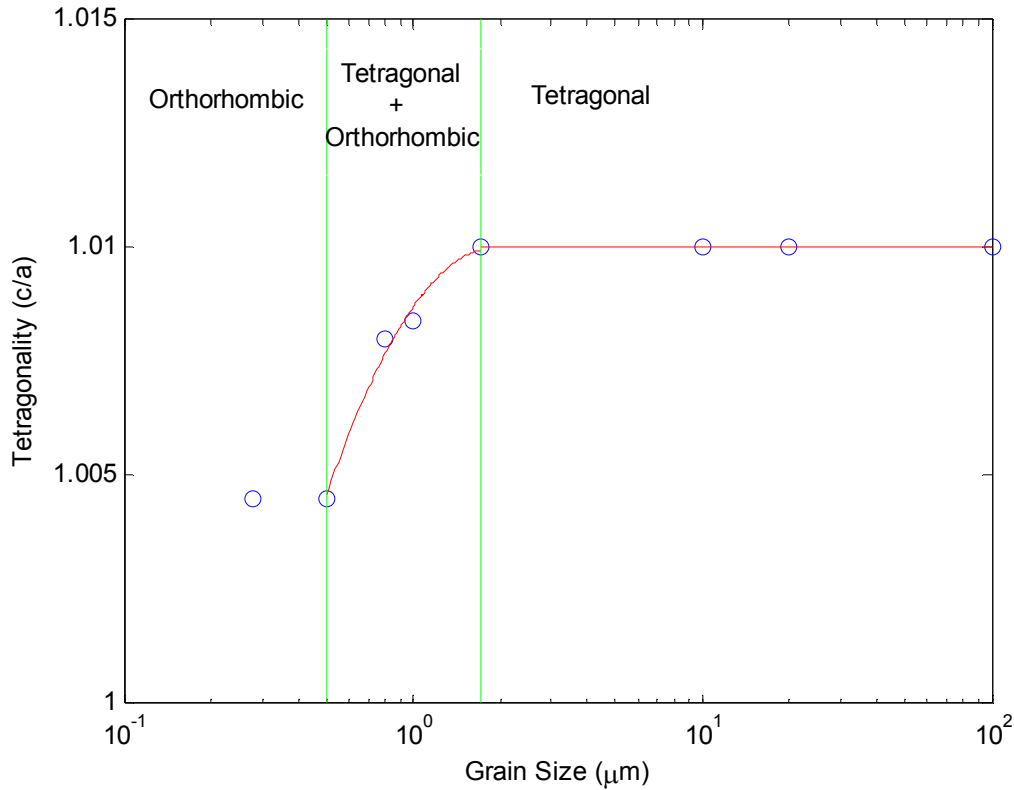


**Figure 4.7 Ratio of tetragonal lattice constants at decreasing grain sizes [Source Arlt et al.]**

While Arlt et al. concluded a peaking in dielectric constant in the range of 0.7 μm to 1.3 μm, in 1989, Shaikh et al. found the peaking to occur at a grain size of about 0.4 μm. Shaikh et al. reported on the dielectric constant of ceramics with a wide range of grain sizes. Their sample construction method, however, yielded ceramics with porosities in the range of 56-90% of theoretical density. The measured dielectric constants were corrected using effective medium theory with coordination number of 6 [14].

A new model was proposed by the authors to predict the dielectric constant at small grain sizes, where previous models break down. This new model approximated the dielectric material as a series / parallel combination of capacitances experienced internal to the grain and at the boundary of the grain. This model did support the data reported by the authors, but has been questioned by later researchers [15].

When the dielectric constant data reported by Shaikh et al. is plotted against that reported by Arlt et al, a correlation is clearly observable. The peak found by Arlt et al. lies in a region of untested grain sizes by Shaikh et al.

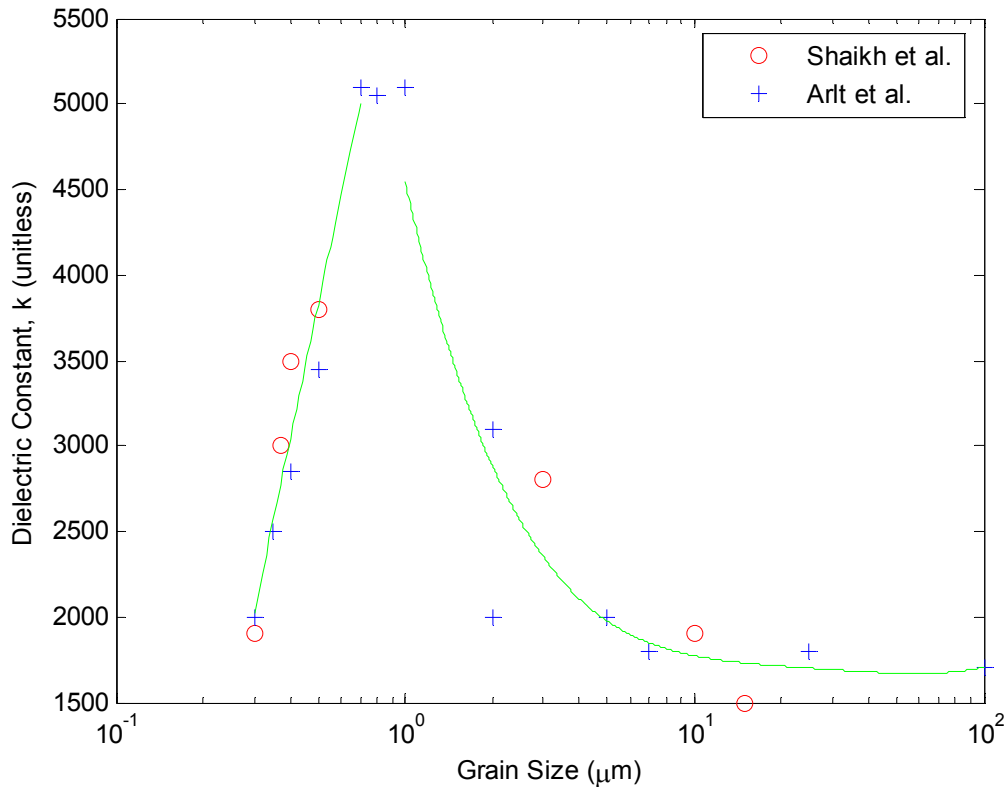


**Figure 4.8 Plot showing the correlation between dielectric constant data found by Arlt et al. and Shaikh et al. [Source Arlt et al. and Shaikh et al.]**

In 1994, Zhong et al. reported on the room temperature crystal structure and temperatures of the phase transitions, monitored by dielectric peaks, for multiple grain sizes. These results are presented in Table 1. From these results, the cubic-tetragonal transition is first evident between grains of 105 and 130 nm in size. These grains showed cubic structure at room temperature. Also included in the table are the room temperature dielectric constants, corrected for porosity. Of note from this data is the disappearance of the phase transitions did not occur simultaneously, but instead in the order rhombohedral-orthorhombic, orthorhombic-tetrahedral, tetrahedral-cubic. Also of note is the porosity of the ceramic samples. These were corrected via effective medium theory to an effective dense ceramic dielectric constant. The authors assumed a 0-3 composite of barium titanate and air for the correction method. This means the barium titanate was assumed a zero dimensional point in a three dimensional space of air.

**Table 4.1 Phase transition temperature and dielectric constant for various grain sizes [Source Leonard, Zhong]**

Grain Size (G) (nm)	% Porosity	Tetragonality (c/a)	Phase Transition Temperature (°C)			Dielectric Constant (K) (25° C)
			R - O	O - T	T - C	
50	45	1	N/A	N/A	N/A	150
105	42	1	N/A	N/A	N/A	200
130	37	1	N/A	N/A	118	400
300	23	1	N/A	29	120	1400
1000	17	1.009	-66	26	121	1900
2000	13	1.011	-71	23	122	1700
4200	9	1.011	-75	20	124	1600
Bulk	N/A	1.011	-80	0	130	N/A

It can be seen from Table 4.1 that the orthorhombic-tetragonal transitional temperature decreases with an increase in grain size. The transitional temperature crosses room temperature for a grain size around 1µm. This transitional temperature corresponds to a peak in dielectric



constant, and by looking solely at the room temperature dielectric constant, the grain size of around 1 $\mu$ m will show a maximum. This coincides with results reported by Arlt et al. in 1985.

In 1996, Leonard compiled his data against previous findings from other authors and found a general trend correlating with the results reported by Arlt et al. for room temperature dielectric constant versus grain size. The compilation is shown in Figure 4.9.

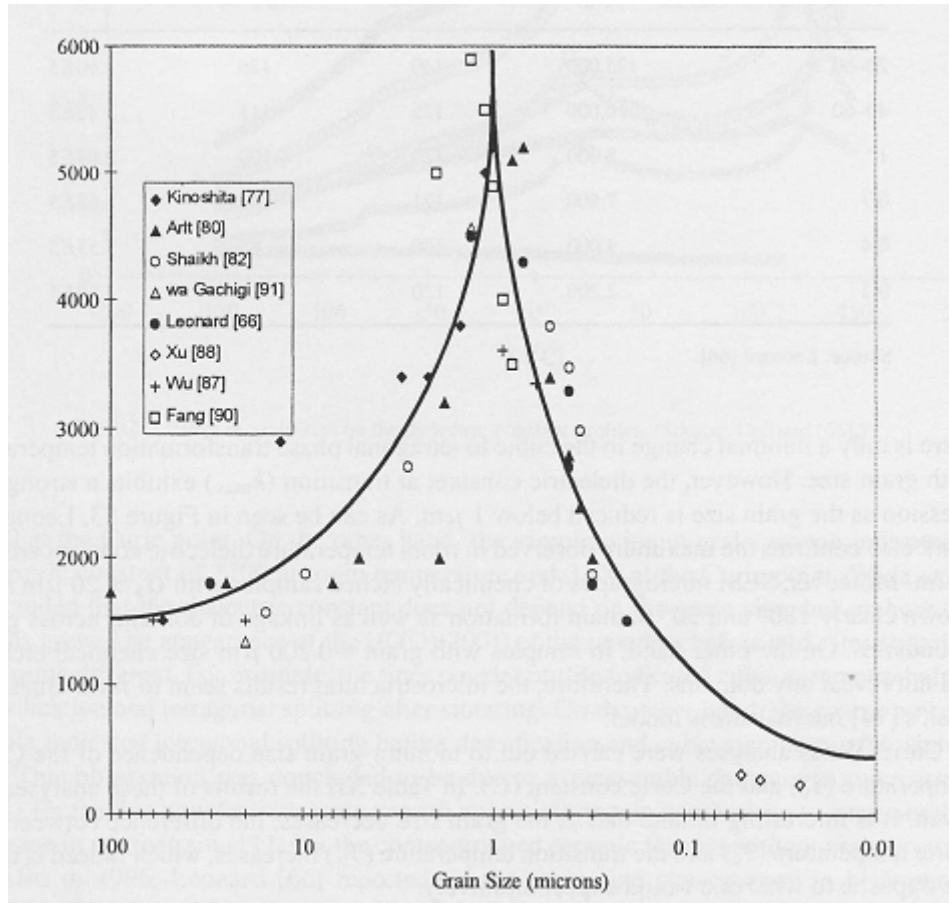


**Figure 4.9** Compilation of various author's findings of dielectric constant at various grain sizes [From Akdogan]

In 2003, Balaraman et al. examined the dielectric relaxation properties of sub-micron (80 nm) grained barium titanate thin films 300nm in thickness. In this publication the authors examined the stability of the dielectric constant at high frequencies up to 8 GHz. These

dielectric constant data were indirectly measured, extracted from high frequency scattering parameters using coplanar waveguide theory. The measured results show dielectric constant stability at frequencies up to 8 GHz and a reduced dissipation factor (as low as 0.07) over bulk or coarse grained material. The authors attribute the high frequency stability to the loss of ferroelectric characteristics in the cubic phase at the small grain size [16].

#### 4.3 Dielectric Constant

Through the history of research on barium titanate material, the dielectric constant has been noted to be affected by a change in grain size. This is due to many factors, each affecting the other, to create a total effect. From the previous section it is difficult to see which factors affect the overall dielectric constant in what way. The following section will single out effects as much as possible for an ease of comprehension.

##### 4.3.1 Internal Stresses

Forces acting on the individual grains originate from, among other sources, the binding of the grains inside the ceramic material. The grains develop 90° domains as a way of alleviating the stresses and equalizing the total system energy [16].

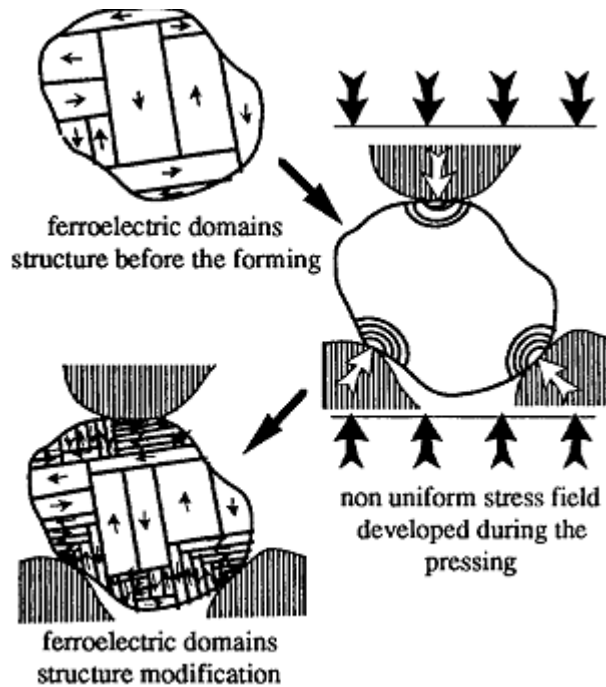


**Figure 4.10 Formation of 90 degree domains due to internal stresses [From Batllo et al.]**

As the grains shrink in size down to the nanometer scale, the crystal structure transitions to a cubic form, abandoning all domain structures in the wake. With the domains absent, the crystal has no way of alleviating the external forces, and exhibits internal stresses, thereby decreasing the total dielectric constant.

#### 4.3.2 Ferroelectric Domains

As grain size decreases, so does the width of the domain walls. These walls were believed to show a minimum size of  $1\mu\text{m}$  and further reduction in grain size would reduce the overall domains. Current theory explains the decrease in domains with size ( $G < 1\mu\text{m}$ ) to be an increase in cumulative domain wall energy becoming too costly compared to the volumetric free energy change of the transformation. Without domain twinning a form of grain clamping occurs where the transformation strain is somewhat suppressed.

#### 4.3.3 Crystal Structure

Four variants of crystal structure exist in barium titanate at different grain sizes. The bulk single crystal structure is tetragonal, yet as the grains are decreased in size, the material goes through a transformation into orthorhombic, then into rhombohedral on its way into cubic. It is in the cubic phase that the material sees its lowest dielectric constant, and each phase shows a decreasing dielectric constant from tetragonal. The transition between two crystal structures shows localized peaks in the dielectric constant [9]. At the Curie temperature the bonds along the lattice structure become increasingly unstable, allowing for dipole alignment and greater lattice vibration, resulting in an increased dielectric constant. This same instability is seen at the other phase transitions [5].

#### 4.3.4 Temperature

As temperature is increased, the dielectric constant follows a pattern determined by the grain size. At grain sizes in the micron range, a well defined peak is seen in the dielectric constant at the Curie temperature and subsequent crystal structure transitional temperatures. As the size of the grains is decreased, these peaks widen and disappear altogether at grain sizes in the nanometer range. This leads to the belief of a temperature – dielectric constant stability for grains in this size range, when in fact the transitional temperatures for crystal structures have been shifted. At a grain size of 20 nm, the Curie temperature has dropped to within the “room temperature” range from 120° C for coarse grained material [10].

#### 4.4 Frequency

The ferroelectric nature of barium titanate yields moveable domain walls that intrinsically provide a hysteresis that impedes high frequency signals. This hysteresis, as a result, causes a dielectric relaxation, reducing the dielectric constant, and high dielectric losses. At grain sizes where the ferroelectric domain effect is the greatest, the relaxation frequency is low. As the

domains are reduced by means of decreasing grain size, this relaxation effect has reduced for testable frequencies resulting in frequency stability for nanometer scale grains [17]. This is most easily seen in Figure 4.11 [17]. The small grain size contains the most ferroelectric domains and thereby experiences a hysteresis effect inhibiting the dielectric constant at frequencies in the GHz range and rolls off to show a lower dielectric constant than the fine grained material.

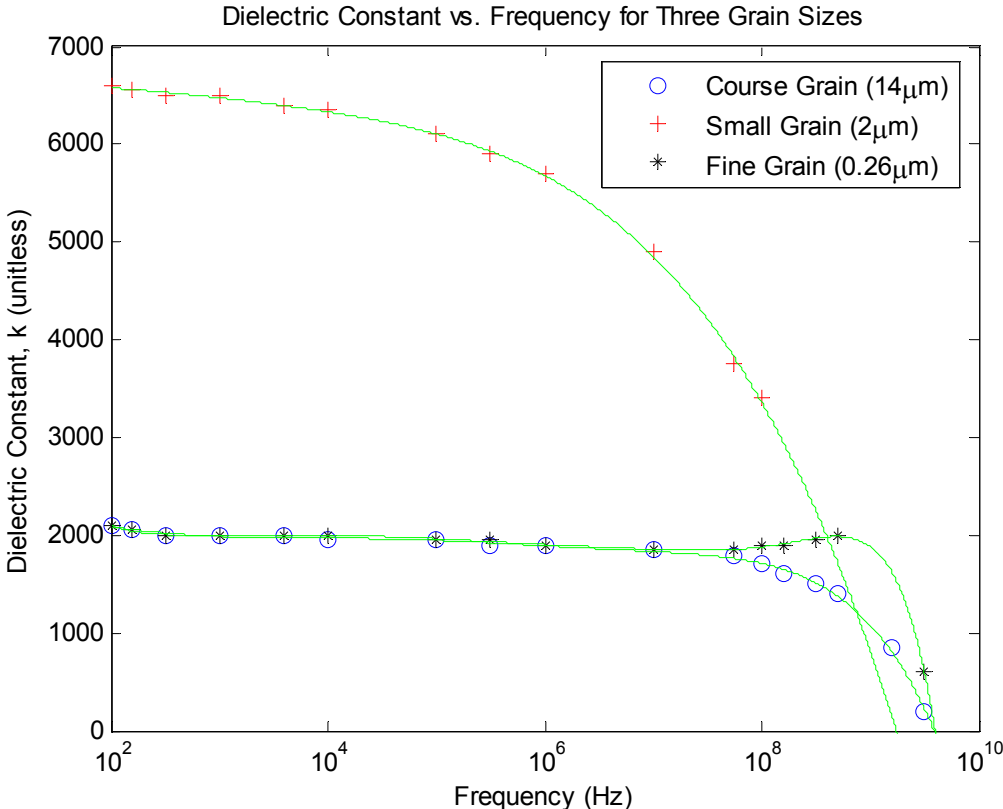


Figure 4.11 Dielectric constant of 3 different grain sizes as frequency is increased [Source McNeal et al.]

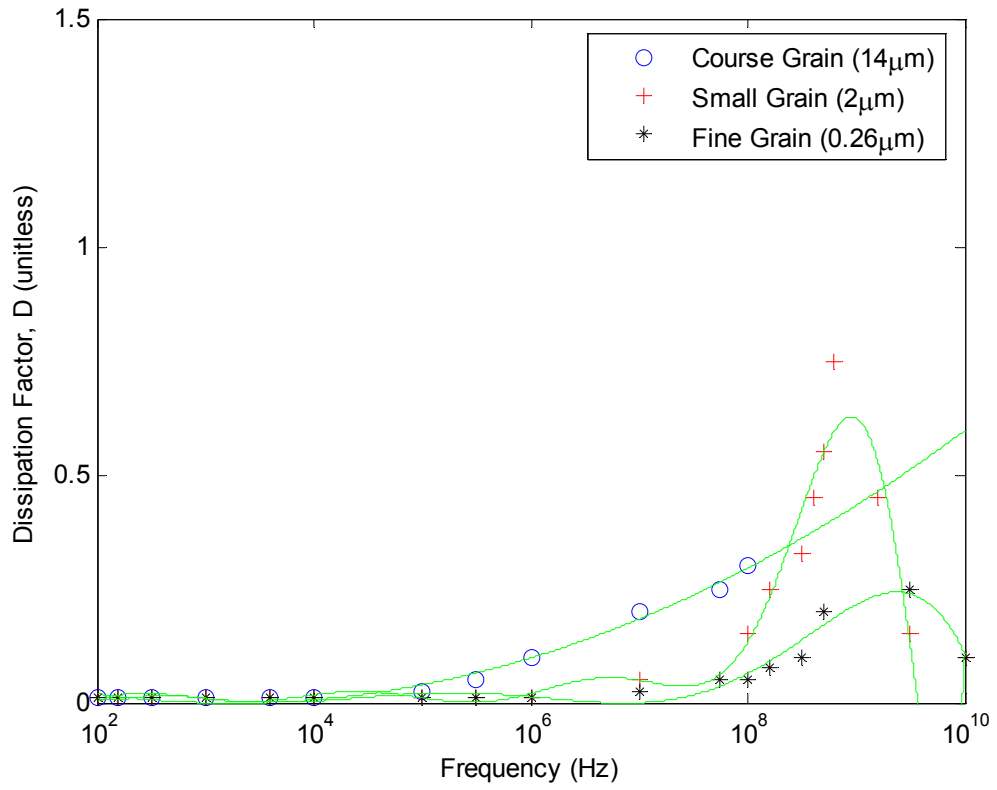


Figure 4.12 Dissipation factor of 3 different grain size materials as frequency is increased [Source McNeal et al.]

## 5.0 Measurement

This section will outline the metrology for barium titanate dielectric material.

### 5.1 Measurement of the Crystal Structure

Since the crystal structure is a determinant of the properties of the material, this is an important metric to characterize. Many methods are available for determination of the crystal structure. This section will discuss the most popular method, XRD.

#### 5.1.1 Crystal Structure Measurement by XRD

X-Ray Diffraction (XRD) has proven a powerful and versatile tool for analysis of many aspects of fabricated barium titanate material. This non-destructive method measures constructively interfered monochromatic x-rays diffracted at specific angles by crystal planes internal to the sample. Through analysis of these diffraction peaks, the crystal structure and the size of the lattice constants can be obtained [18]. This measurement can be performed on both powder and sintered ceramic samples.

#### *Theory of Operation*

X-Rays are emitted toward the device under test (DUT) by means of electron bombardment of a copper plate. This emits  $\text{CuK}\alpha$  rays which have a narrow spectral energy, of large enough amplitude to produce a wavelength small enough to penetrate the crystal structure of the DUT. As these rays strike the first crystal plane diffraction occurs, and a certain portion of the waves are reflected off of the first crystal plane while some of the rays penetrate the first layer and reflect on the second crystal plane, and so on [19].

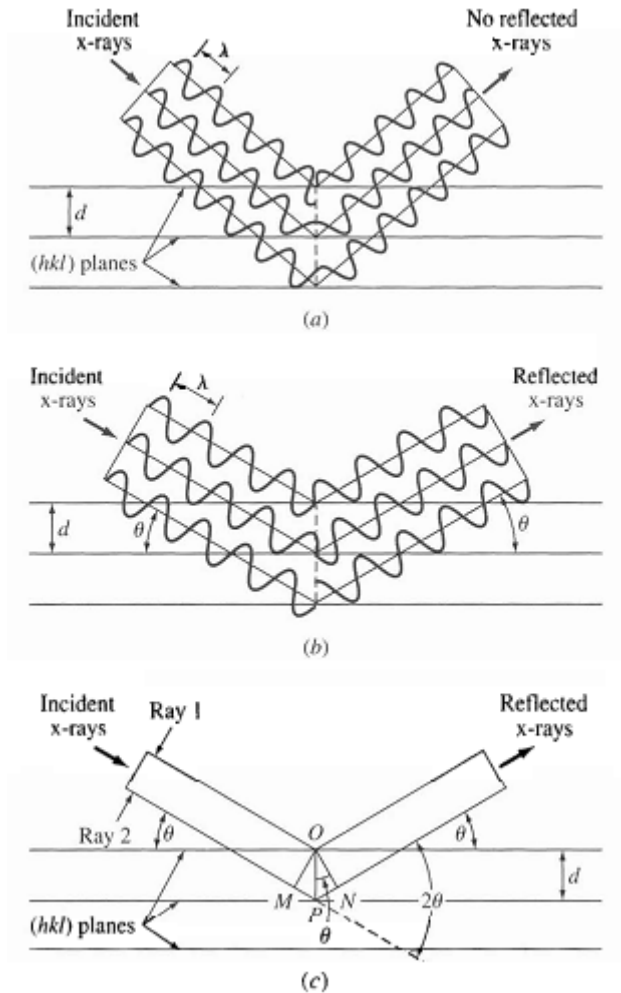


**Figure 5.1 Example of x-ray diffraction where in a) the angle of rotation yields a destructive interference pattern, but in b) the angle yields a constructive interference pattern. Figure c) shows the measurement of the Bragg angle [From Smith and Hashemi]**

If these planes are separated by a distance that is a factor of the wavelength of the X-ray, they constructively interfere creating a larger energy which is picked up by the receiver. The DUT is rotated through  $\theta$  degrees (up to 180) and these interference patterns are displayed on a graph. From Bragg's law the distance between planes can be found.

$$n\lambda = 2d \sin \theta \quad (5.1)$$



In this equation, the integer  $n$  is referred to as the order of the corresponding reflection,  $\lambda$  is the wavelength of the reflecting X-ray, and  $d$  is the distance between lattice planes [20].

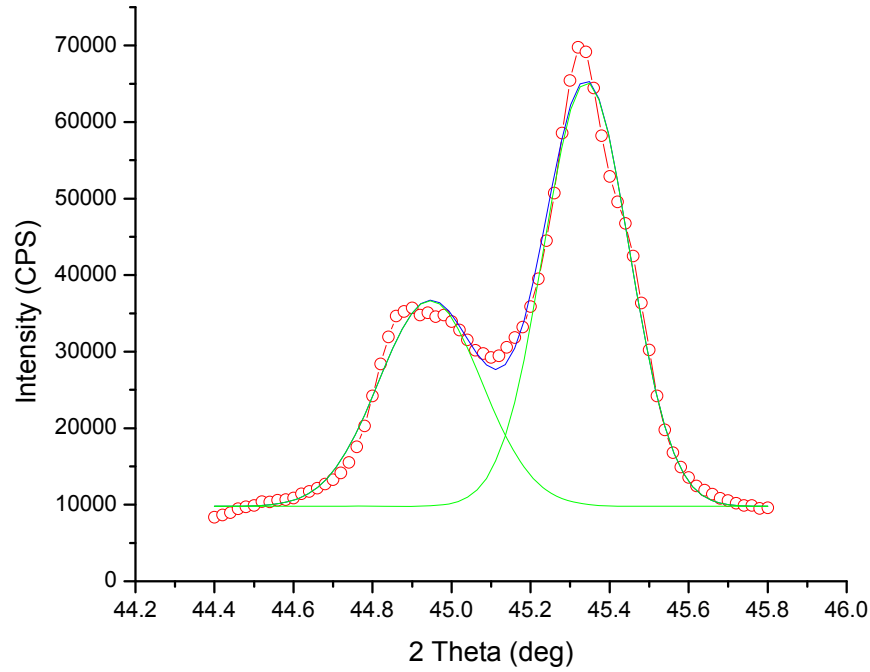


**Figure 5.2 Sample XRD plot showing diffraction peaks at 44.9 and 45.4 degrees ( $2\theta$ ) [Source Nanoscale]**

Figure 5.2 shows a sample diffraction pattern for barium titanate. This plot shows the peaks corresponding to the  $a$  and  $c$  axis lattice constants. This peak splitting shows a tetragonal crystal structure. If the structure were cubic in nature the peaks would align.

By examining the  $n = 2$  plane, the peaks can be resolved better into the individual contributions of the overall shape. This can prove extremely useful when the phase is transitioning from tetragonal to cubic [19].

## 5.2 Measurement of Grain Size / Powder Size

It is extremely important to understand the size of the individual grains or powder crystallites. Several methods have been used to characterize this dimension; however this section will only discuss two of these methods.

#### 5.2.1 Measurement of Size by XRD

Grain size measurement is yet another application of the XRD measurement. This technique has been widely used and documented. By measuring the grain size through XRD the need for other expensive equipment is eliminated as the XRD can be used for multiple analysis techniques.

##### *Theory of operation*

As the size of the individual grain or powder crystallite that is being tested decreases, the width of the diffraction peak in the XRD plot increases. This increase in width is predictable through the use of Scherrer's equation. Through this analysis, the width of the diffraction peak is measured at full width, half maximum (FWHM), meaning the full width of the peak is measured at half the amplitude between the minimum and maximum [21] as shown in Figure 5.3.

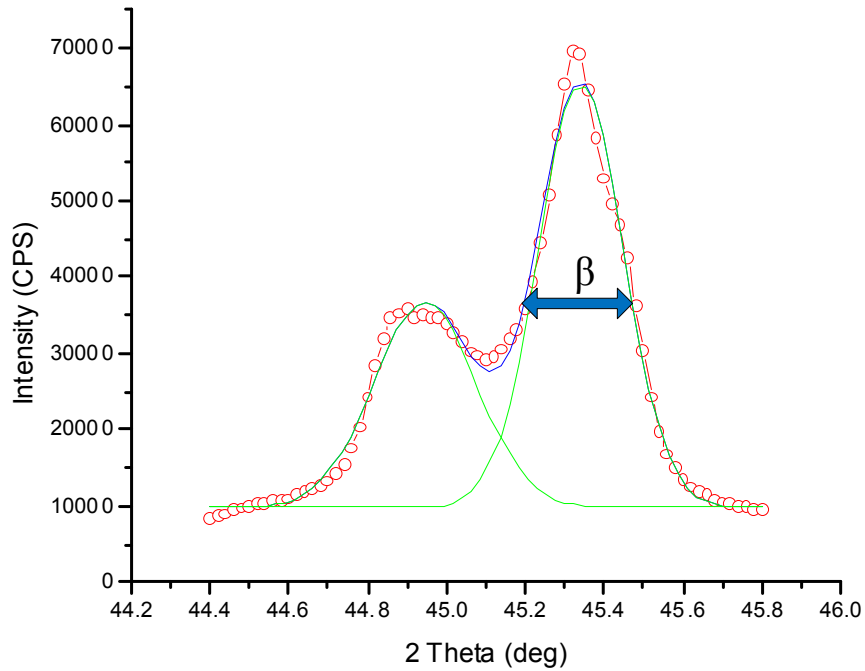


**Figure 5.3 Example XRD plot showing the full width half maximum measurement beta for use in grain size analysis [From Nanoscale]**

This FWHM distance ( $\beta$ ) is then used in the following equation:

$$D = \frac{K\lambda}{\beta \cos(\theta)} \quad (5.2)$$

In this equation, D is the particle diameter, K is the Scherrer constant (K=0.9),  $\lambda$  is the X-ray's wavelength, and  $\theta$  is the diffraction angle.

This simple method based on Scherrer's equation is only valid if internal stresses are not present. If these stresses do exist, the method for finding the grain size becomes a little more complex. The most common method is based upon the realization that the broadening of the peak is due to both the decrease in grain size and the stresses, which have different angular

relationships. The broadening described in the Scherrer equation has a relationship of  $\frac{1}{\cos(\theta)}$  whereas the strain follows a  $\tan(\theta)$  relationship. The instrumentation also lends to peak broadening. Therefore the total broadening can be found by the following equation.

$$\beta_{Total}^2 \approx \left[ \frac{K\lambda}{D \cos(\theta)} \right]^2 + [4\varepsilon \tan(\theta)]^2 + \beta_{Inst}^2 \quad (5.3)$$

In this equation,  $\varepsilon$  is the strain and  $\beta_{Inst}$  is the broadening due to the instrument. Through a least square fit method of several experimentally found  $\beta$  values, both the strain and the grain size can be solved for at the same time [21].

### 5.2.2 Measurement of Size by SEM

Measuring the size of the individual grains is a little removed by use of XRD, relying on diffraction peak spreading. With a scanning electron microscope (SEM), the individual grains can actually be seen and measured with the human eye.

#### *Theory of operation*

While normal optical microscopes rely on light and lenses to bring a picture of the sample to the operator, the SEM scans the sample with a beam of electrons, allowing for very high resolution [22]. This very narrow beam, providing a resolution in the angstrom range, is scanned side to side, one row at a time. The backscattered electrons from the sample are received and an image is processed.

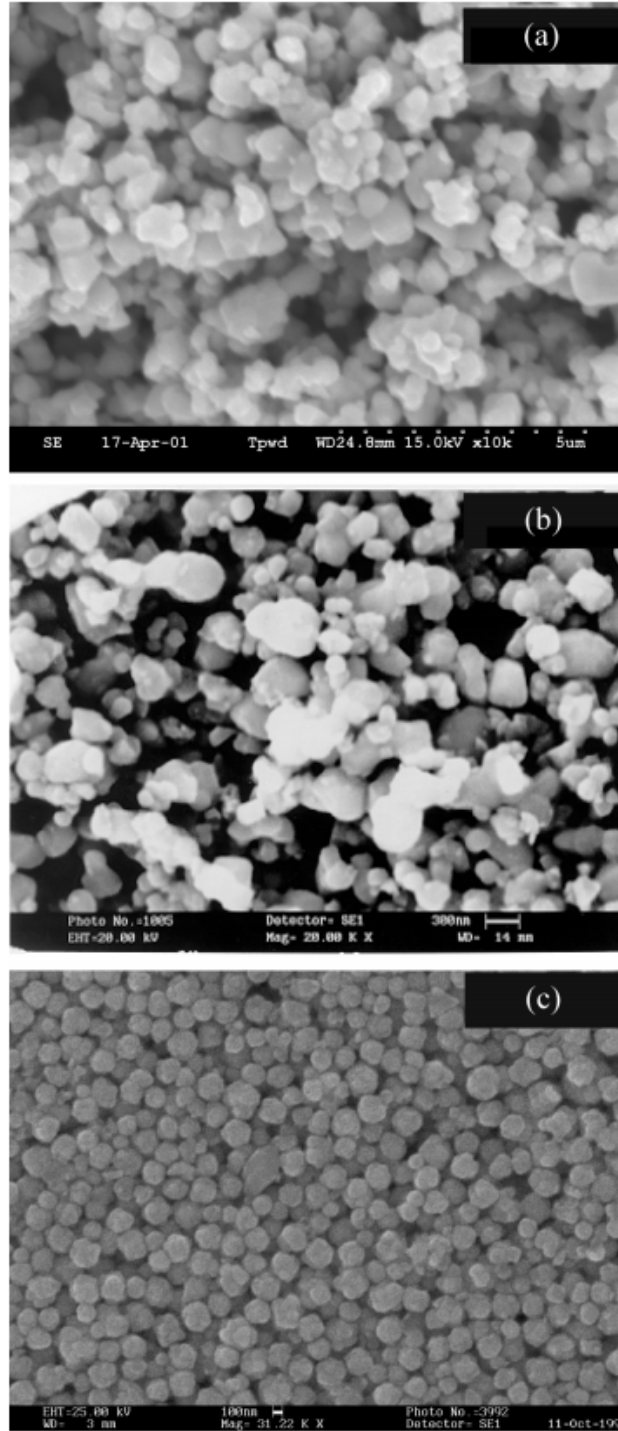


**Figure 5.4 SEM images of barium titanate powder produced by 3 different methods [From Yoon et al.]**

With such a fine resolution, the individual grains can be measured by visual methods. Multiple grains should be measured and averaged for a final size dimension.

### 5.3 Dielectric Measurement

The dielectric properties of the barium titanate material are of utmost concern. These properties are generally measured on sintered ceramics of ideal density, and this is where the majority of the discussion lies, but recently a method has been proposed for measurement of the dielectric properties of the material in powder form.

### 5.3.1 Pellet Construction

In order to measure the dielectric properties of the barium titanate material, it is imperative to have a quality ceramic pellet. With defects in the sample, the measurements are of questionable accuracy. Many considerations need to be taken into account for quality test samples.

#### *Porosity*

Less than 100% ideal porosity has been shown to affect the overall dielectric constant of the material [23]. This is partially due to the fact that the dielectric is no longer comprised of barium titanate in a porous material, it should be considered a [0-3] composite of barium titanate in air [23]. This means the system is comprised of zero dimensional points of barium titanate in a three dimensional space of air. With the system a mixture of two very different dielectric constants (air having a dielectric constant of 1.004), the overall dielectric constant is reduced by a large factor. Zhong et al. showed this effect can be corrected using the effective medium theory. Secondly the internal stresses on the grains have been shown to increase dielectric constant [9]. These stresses occur when the grain is compressed by neighboring grains. In porous samples, these grains may not have this compression stress.

#### *Sintering process*

Many different processes have been reported by authors, but one trend remains: a higher sintering temperature yields a larger grain size. Table 5.1 shows sintering temperatures and resulting grain sizes as reported by various authors.

**Table 5.1 Sintering conditions and resulting grain size and porosity as reported by various authors [Source: authors listed]**

Author	Year	Temperature (° C)	Time (Hr)	Grain Size (µm)	Porosity (%)	Other Factors
Arlt	1985	1100	0.25	.3 - .5	0.1	2 GPa pressure
Zhong	1994	750	2	0.05	45	
Zhong	1994	800	2	0.105	42	
Zhong	1994	900	2	0.13	37	
Zhong	1994	1000	2	0.3	23	
Zhong	1994	1150	2	1	17	
Zhong	1994	1250	2	2	13	
Zhong	1994	1350	2	4.2	9	
Shaikh	1989	1050	0.5	0.3	> 0	
Shaikh	1989	1100	0.5	0.35	> 0	
Shaikh	1989	1150	0.5	0.4	> 0	
Shaikh	1989	1200	0.5	0.5	> 0	
Shaikh	1989	1225	0.5	2.8	> 0	
Shaikh	1989	1300	5 min	9.6	> 0	
Shaikh	1989	1300	0.5	15.5	> 0	
Frey	1997	900	0.5	0.09	2	

The porosity has been decreased for those ceramics sintered under pressure in a Hot Isostatic Press. Arlt et al. reported a 99.9% ideal density by compressing the material without

binder at 2 GPa and then heating it under a reduced pressure [9]. Authors not included in this table did not report the sintering procedure.

### 5.3.2 Measuring Dielectric Constant

The dielectric constant can easily be measured for a sintered ceramic by use of an LCR meter, however until recently no accurate method was found to measure the dielectric constant of the powder form, when Ohno et al. used Raman Spectroscopy to extrapolate the dielectric constant. This section will discuss both methods.

#### *LCR Meter*

This is the most widely used instrument in dielectric testing on a small scale. It provides an “all-in-one” approach to capacitance measurement. The instrument can measure capacitance and parasitic resistance, and the dielectric constant can easily be calculated if the physical dimensions of the parallel plate capacitor are known.

#### *Theory of Operation*

By applying a small sinusoidal signal of frequency  $f$  and amplitude  $A$  to the capacitor, the LCR meter can measure the voltage ( $V$ ) across the capacitor and the displacement current ( $I$ ) through the capacitor and find the complex impedance ( $Z$ ) from Ohm’s Law.

$$\frac{V}{I} = Z = R - jX = Z \angle \theta^\circ \quad (5.4)$$

$$X = \frac{1}{2\pi fC} \quad (5.5)$$

If the capacitance under test is small the reactance  $X$  is large, and more likely to be affected by a parallel parasitic resistance. If the capacitance under test is large, the reactance is small and more likely to be affected by a series resistance. The capacitances seen in



measurement were quite small, and the parallel resistance model was more fitting, so it will be discussed over the series resistance model.

To make the math easier, the admittance (Y) is found instead of the impedance.

$$\frac{I}{V} = \frac{1}{Z} = Y \quad (5.6)$$

$$Y = G + jB = Y \angle \phi^\circ \quad (5.7)$$

$$|Y| = \sqrt{G^2 + B^2} \quad (5.8)$$

$$B = 2\pi fC \quad (5.9)$$

$$R_p = \frac{1}{G} \quad (5.10)$$

In these equations, G is the conductance, measured in Siemens, and B is the susceptance, also measured in Siemens. All this math is done inside the LCR meter, and the capacitance (C) is displayed along with the parasitic parallel resistance ( $R_p$ ). Also useful are the quality factor (Q) and the dissipation factor (D). These provide a metric for the ratio of parasitic resistance and capacitance [3].

$$Q = \frac{1}{D} = \frac{|B|}{G} \quad (5.11)$$

If the capacitor were ideal, no parasitic resistance would exist and the quality factor would be infinite. From this a high quality factor, or low dissipation factor, is desirable.

Once the capacitance is found, the dielectric constant can be easily calculated by back solving the parallel plate capacitor equation.

$$\varepsilon_r = \frac{Cd}{\varepsilon_0 A} \quad (5.12)$$

By adding a DC offset voltage, the internal ferroelectric domains can be polarized, thereby studying the effect of polarization on the dielectric constant.

### ***Raman Spectroscopy***

Raman spectroscopy, like XRD, has proven a very powerful tool in the analysis of many different aspects of barium titanate. This process has been used to determine the crystal structure, but has not proven as popular as XRD in this respect. Recently the Raman method has been successfully used to determine dielectric constant for loose powder barium titanate [10].

#### *Theory of operation*

Whereas XRD bombards X-rays at the sample reflecting from the lattice planes, Raman spectroscopy bombards the sample with photons in the form of a monochromatic laser. These photons interact with the electron cloud of the atoms as they pass through the crystal structure. When the photons interact with these electron clouds, the atoms begin to vibrate, consuming some of the incident photon's energy in the process. The vibrational modes of the atoms interfere with the incoming laser beam causing a shift in the light frequency. This difference in frequency translates to a different wavelength of light being received. The intensity of the received light is then plotted against the received light's wavelength difference from the incident beam [24].

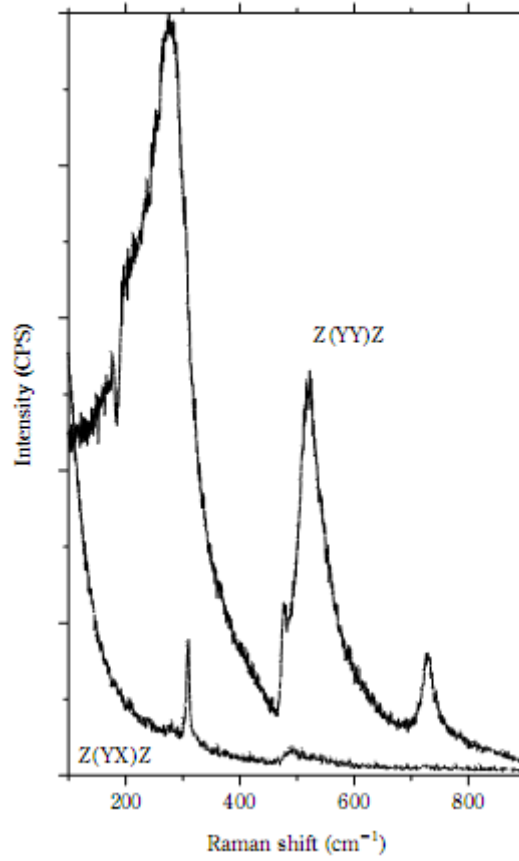


**Figure 5.5 Sample Raman spectra plot for single crystal barium titanate [From Ohno et al.]**

The electron vibration occurs in two forms, longitudinal optical (LO) and transverse optical (TO). Using the peaks of each vibration, the dielectric constant can be found.

$$\frac{\epsilon}{\epsilon_{\infty}} = \frac{\omega_{1LO}^2}{\omega_{1TO}^2} * \frac{\omega_{2LO}^2}{\omega_{2TO}^2} * \frac{\omega_{3LO}^2}{\omega_{3TO}^2} \quad (5.13)$$

where  $\omega$  is the mode frequency for each phonon mode, and  $\epsilon_{\infty}$  is the optical dielectric constant (a = 5.22 and c = 5.07) [10].

### 5.3.3 Measurement of Temperature Dependence

It has been shown in previous sections that the dielectric constant of barium titanate depends heavily on the temperature at which it is measured. This can easily be measured

through use of the LCR meter and a temperature chamber with the LCR meter set statically and only temperature varied.

#### 5.3.4 DC Resistance

Ideally, no electrical connection should exist between the two plates of a parallel plate capacitor, the dielectric acting as an insulator at DC. If a small DC voltage produces a current through the capacitor, the sample is not a quality product and should be discarded. Defects in production may cause this leakage current. This test can provide a first line defense for catching bad samples.

##### *Theory of Operation*

Like the LCR meter discussed previously, the digital multi-meter (DMM) in resistance mode sources a test current to the sample and measures the voltage across it. In 2-wire resistance mode, only two probes are used, and the current is sourced on the same probes as voltage is measured. Through Ohm's Law, the measured voltage (V) and source current (I) are used to calculate the resistance.

$$\begin{aligned} V &= IR \\ R &= \frac{V}{I} \end{aligned} \tag{5.14}$$

The two wire measurement is not as accurate as the 4 wire method, which sources current on a different set of probes than the probes on which voltage is measured. Ideally the current through the capacitor should be zero, resulting in an infinite resistance, so accuracy isn't imperative at this point.

#### 5.3.5 Dielectric Strength

An important metric of the dielectric material is the dielectric strength, also called the breakdown voltage. Generally this is a destructive test as part of the atomic structure of the

dielectric material is altered. Caution should be taken as the voltage required for breakdown is quite large and upon breakdown the release of energy can be large enough to destroy the device in an explosive manner.

### *Theory*

When the voltage across a dielectric is large enough, electrons become stripped from the nuclei, thereby ionizing some or all of the atoms in the dielectric [2]. The minimum voltage at which this occurs is referred to as the dielectric breakdown voltage and is dependent on the distance between the two electrodes. To measure the breakdown point, a DC voltage should be applied across the device and increased slowly until a sudden increase in current is seen.

Barium titanate has shown the breakdown voltage to be independent of temperature in the ferroelectric phase, but does have minimum peaks at the phase transitional temperatures [25].

### 5.3.6 Industry Testing

On a production line, the concern is not with fully characterizing the dielectric material as much as it is with ensuring the product is of quality and meeting standards specifications. Therefore the tests are less involved than those performed in the laboratory setting. Normally the capacitance and loss factors are measured at 1V AC and 1 kHz. The temperature characteristics are also verified for the range as stated by the standard (from -55°C to 125°C for X7R standard). Dielectric breakdown voltage is also verified in the form of testing a manufacturer's recommended maximum voltage, for quality purposes [26].

## 6.0 Measurement Results

Samples were prepared by Nanoscale Corporation in Manhattan, KS through a proprietary process. The resulting barium titanate powder yielded crystallite sizes in the range of 11 nm and 33 nm as measured by XRD. A sample XRD plot with  $2\theta$  measured from  $0^\circ$  to  $90^\circ$  is shown below.

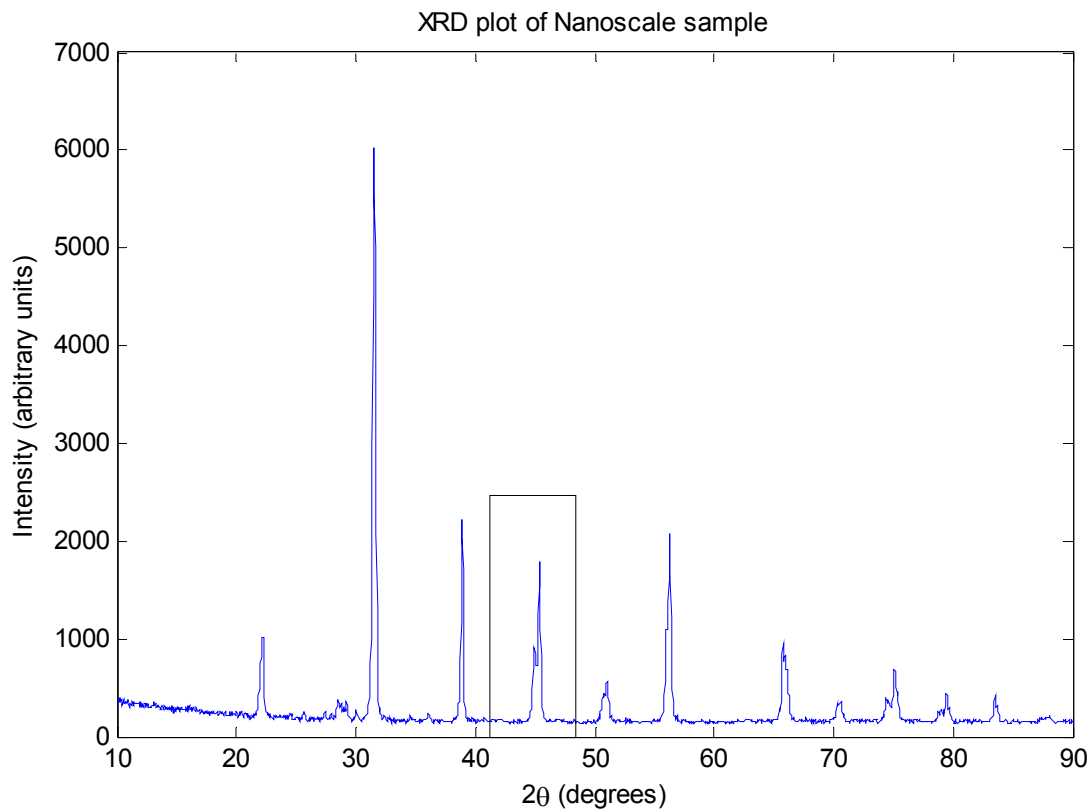


**Figure 6.1 XRD plot of sample from Nanoscale measured from 0 to 90 degrees**

The rectangle marks the zoomed in  $2\theta$  region shown in Figure 6.1. In this region, the  $\langle 200 \rangle$  and  $\langle 002 \rangle$  planes can be seen in greater detail and measured for tetragonality.

Tetragonality was verified and the powder size was measured to be in the range of 11 nm to 33 nm with agglomerated groups of about  $0.7 \mu\text{m}$  in size.

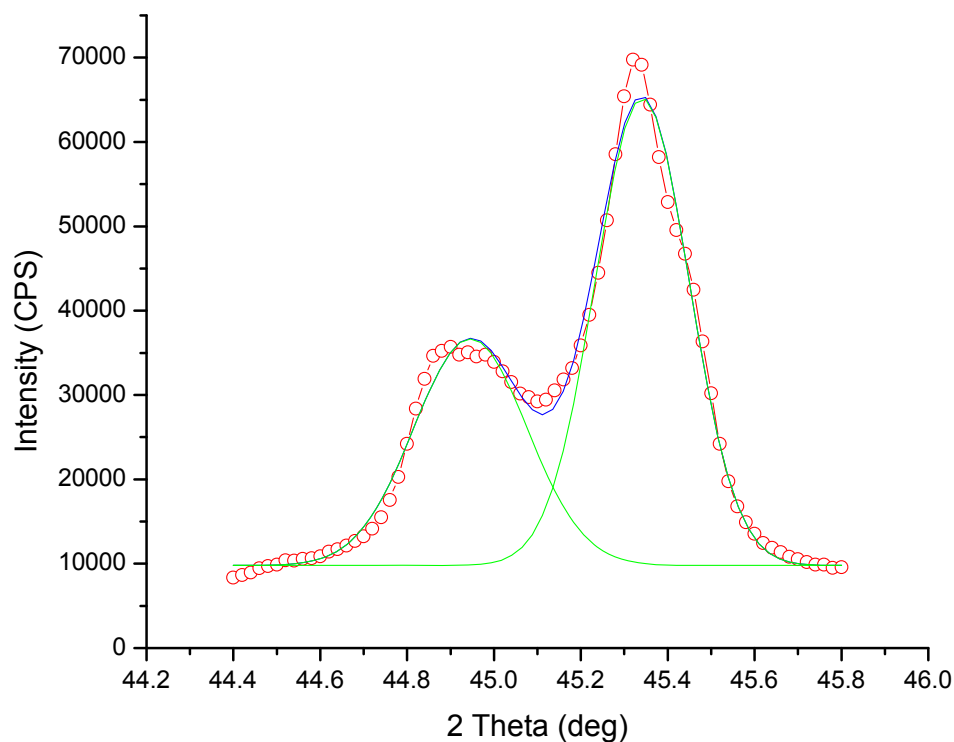


**Figure 6.2 Sample XRD plot from 44 degrees to 46 degrees showing tetragonality in <200> and <002> planes**

**[From Nanoscale]**

To measure the dielectric properties, the powder was formed into pellets through pressing with binder at room temperature, without sintering. Electrodes were painted on the ends with a silver paste and then copper leads were painted on over the electrodes. The entire assembly was coated in wax to hold the form throughout transport and testing.

The dielectric constant was measured using an HP 4284A LCR meter through a frequency range of 100Hz to 1MHz and amplitude of 50 mV. The resulting measured capacitance values were then used to calculate the dielectric constant. The figure below shows the dielectric constant of several samples created by varying chemical reaction conditions.

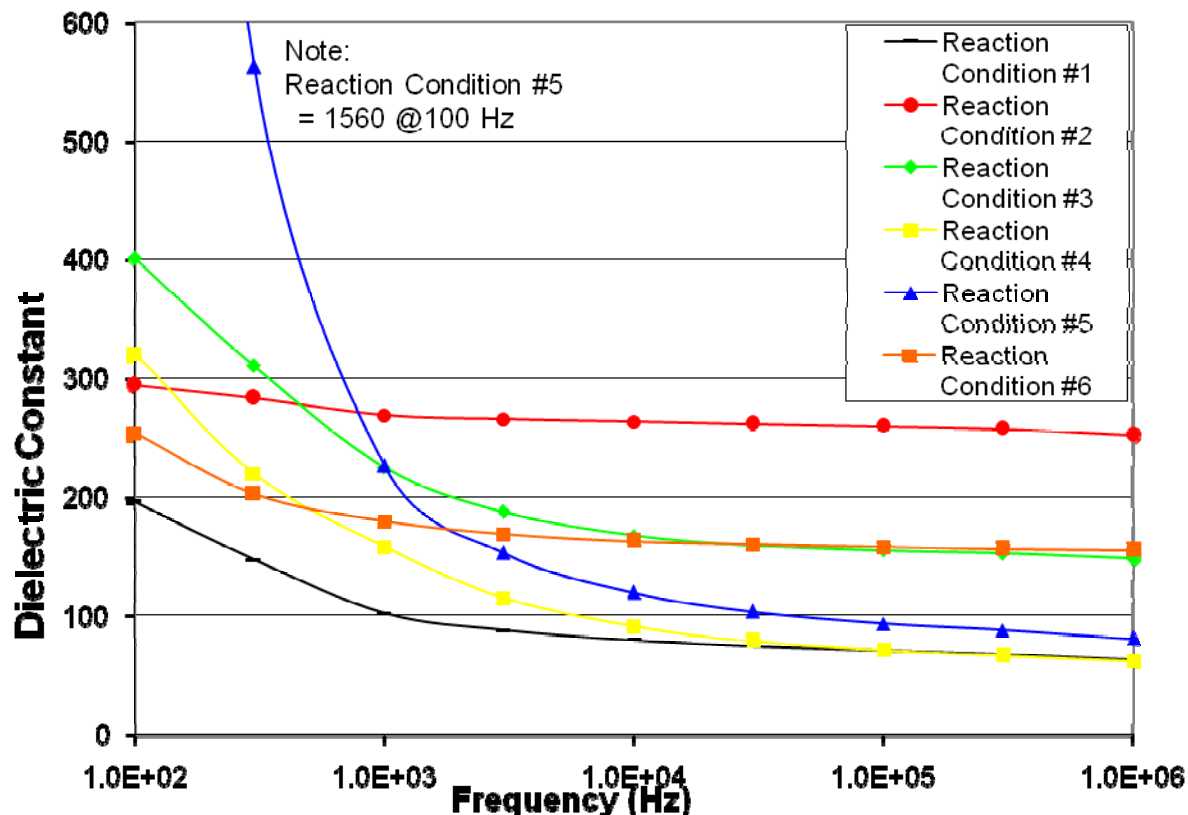


Figure 6.3 Measured dielectric constant for various reaction conditions [Source Nanoscale Corp.]

The dielectric constant for these samples shows frequency instability at lower frequencies. This contradicts McNeal et al. who showed dielectric constant stability through the GHz range. The dielectric constant seems to be low compared to the results reported by Ohno et al, though they used a different measurement method.

The dissipation factor was also recorded from the LCR meter at various frequencies and plotted in Figure 6.4. The various reaction conditions yield quite different dissipation factors. Each of the samples shows a dissipation factor dependent on frequency. The high dissipation factor of reaction condition #1 show the sample was more lossy than it was capacitive at low frequencies which is an undesirable quality. In the MHz range, each of the lines seem to



converge at a low dissipation factor, showing a high frequency stability in the samples, which agrees with the dielectric constant measurements.

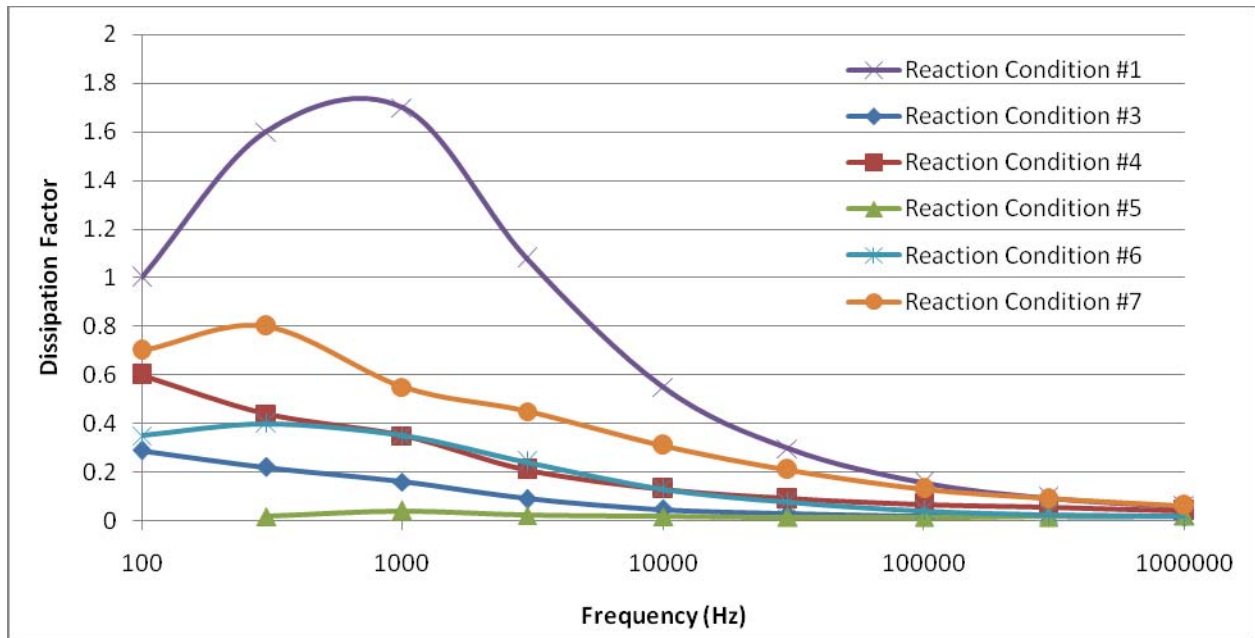


**Figure 6.4 Measured dissipation factors for various reaction conditions [Source Nanoscale Corp.]**

After these measurements were taken, the porosity was determined to be about 70%, or the samples were only 30% of the ideal theoretical density which may explain the dielectric constant measurement results. The measured dielectric constant values were corrected via the effective medium theory assuming a 0-3 composite of barium titanate and air, only to get unreasonable results. The assumption of a 0-3 composite was probably invalid with this porosity level.

The HP4284A LCR meter is capable of applying a dc bias voltage to the samples to test for polarization. When DC levels from -10V to +10V were applied no effect was seen.

## 7.0 Conclusion and Future Work

Barium titanate has proven to be a versatile dielectric material. However, with a decrease in the individual powder size, many problems arise. Assuming an end application as a dielectric material in capacitive constructions, the largest problem encountered with a decrease in size is the variation in dielectric constant. Shrinking the size of the grain in a sintered ceramic shows an increase in dielectric constant down in to the micron range. The peak has been shown to occur anywhere from 1 micron to 0.7 micron grain size [Arlt et al]. Further decrease shows an adverse effect with the trend following a quadratic fall, eventually lying on an asymptote at a dielectric constant of about 400 [Akdogan]. While Ohno et al. did find a sharp increase in the dielectric constant of a powder with sizes in the nanometer range, sintering processes increase the size of the grains to a dimension well above this phenomenon.

The decrease in dielectric constant is partially due to the decrease in ferroelectric domains. As the grains decrease, the domains disappear due to the phase transition between tetragonal and orthorhombic crystal structures. The tetragonal structure has the titanium ion shifted slightly upwards in the unit cell along the  $c$  axis, producing a natural ferroelectric domain. As the transition occurs toward a orthorhombic structure, the  $c$  axis decreases to the same dimensionality as the  $a$  and  $b$  axes. The alignment of these ferroelectric domains with an external field yields a high dielectric constant.

The dielectric constant has a natural temperature response that is also affected by a decrease in grain size. The dielectric constant shows peaks at temperatures corresponding to each phase transition. With a decrease in grain size, the transitional temperatures shift. At a grain size in the range of 0.7 microns to 1 micron, the orthorhombic-tetragonal phase transition temperature resides at room temperature, causing a sharp increase in room temperature dielectric

constant. This sharp increase in dielectric constant brings with it a larger temperature coefficient of capacitance, meaning any change in temperature will generate a change in the dielectric constant, which in turn changes the overall capacitance of the device. Ohno et al. found powders in the 20 nm range showed a large increase in dielectric constant due to the Curie temperature dropping to the room temperature range. At the Curie temperature, the tetragonal bonds in the unit cell become unstable as the crystal transitions into a cubic form. This instability brings with it a large, sharp dielectric constant peak. At the Curie point, the temperature coefficient of capacitance will likely be quite high; the slightest change in temperature will drop the capacitance a significant amount.

Even with all these negative effects, decreasing the grain size can yield a high volumetric efficiency (capacitance per unit volume). By decreasing the grain sizes, the ability to create a thinner dielectric layer inside a multilayer ceramic capacitor arises. Since each layer is in parallel, the total capacitance is number of layers multiplied by the capacitance seen by each layer. With a constant electrode plate area, the only determinant of capacitance per layer is the dielectric constant.

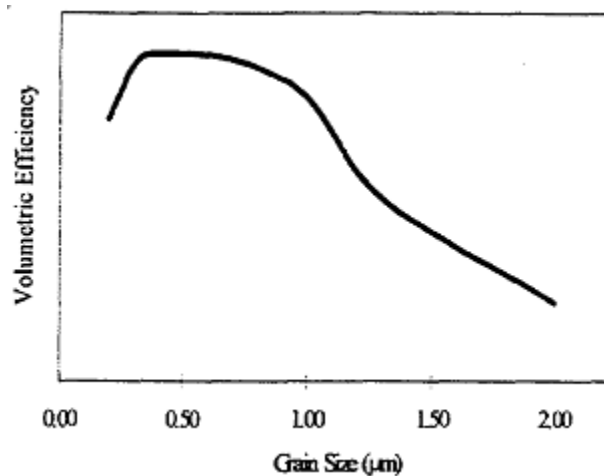


Figure 7.1 Volumetric efficiency per with variation in grain size [From Leonard et al.]

## 7.1 Future Work

There is much work to be done on this project still. The future work can be classified into three parts that need equal attention. Each part is essential to the success of the project as a whole.

### 7.1.1 Pellet production

In order to get quality measurements, the barium titanate must be processed into a quality sintered ceramic pellet sample. A “good quality pellet” is a blanket term that encompasses many factors. First and foremost the powder used to generate the pellet must be fully reacted material. If any material is left unreacted, the dielectric properties could be thrown off completely as pure barium or pure titania have separate dielectric characteristics than the reacted barium titanate. This fact has been assumed in previous discussions, but must still be ensured for quality measurements. Secondly the sintered pellet sample must be as near as possible to theoretical density. This has been the greatest hurdle to this point for samples produced by Nanoscale Corporation. They are not alone in this, many previous researchers reported sub-optimum porosity levels that have been mathematically corrected afterwards. If porous cavities exist internal to the sintered ceramic sample the dielectric characteristics are no longer descriptive of pure barium titanate, but for a combination of materials. This can lead to erroneous measurement results and conclusions.

### 7.1.2 Characterization

Once quality sintered ceramic pellet samples have been produced, dielectric characterization can be done through methods described previously. Though measurement of the dielectric constant over a range of frequency was performed on previous samples, the validity of the data at the end was questionable. These measurements will need to be performed again to

verify the characteristics. At the same time, the dielectric breakdown voltage can be measured. Previously it was almost too weak to be accurately measured by the Stanford Research high voltage supply. This was attributed to the sample quality. Tests that were not performed previously and will need to be in the future include temperature characterization. A temperature chamber that can both heat and cool should be used to vary the temperature of the barium titanate sample over a wide range while measuring the dielectric constant at a static frequency. This test should reveal a temperature profile that will determine the temperature coefficient of capacitance (TCC). After this is found, a verification can be made on the adherence to the set IEC standards for MLCC ceramic dielectric material. These standards regulate temperature characteristics as well as a minimum dissipation factor, among other things.

#### 7.1.3 Scale powder production

The end goal for this project is to make a dielectric material for production capacitors. The current method for production of the powder can't create enough to support a retail production. Work will be needed to increase production of the material enough to support expected sales. This area of the project is beyond the scope of the research put forth for this report.

## 8.0 References

- [1] E. K. Akdogan, M. R. Leonard and A. Safari, "Size Effects in Ferroelectric Ceramics,"
- [2] K. Demarest, *Engineering Electromagnetics*. Prentice Hall, 1997,
- [3] Anonymous "Agilent 4248A precision LCR meter operation manual," Agilent Technologies, Japan, 2001.
- [4] H. Egebo, "Electrolytic Capacitors: A Beginner's Guide," vol. 2007,
- [5] D. Yoon and B. Lee, "BaTiO<sub>3</sub> properties and powder characteristics for ceramic capacitors," *Journal of Ceramic Processing Research*, vol. 3, pp. 41, 2002.
- [6] Epcos, "Technical information: MLCC," Epcos AG, Munich, Germany, 2002.
- [7] A. Safari, R. Panda and V. Janas. (2000, Ferroelectric ceramics: Processing, properties and applications. *Published Online at: [Http://www. Rci. Rutgers. edu/~ecerg/projects/ferroelectric. Html](http://www.Rci.Rutgers.edu/~ecerg/projects/ferroelectric.Html)* (11/28), pp. 59. Available: <http://www.rci.rutgers.edu/~ecerg/projects/ferroelectric.html>
- [8] B. Carlberg, J. Norberg and J. Liu. (2007, Electrospun nano-fibrous polymer films with barium titanate nanoparticles for embedded capacitor applications. *IEEE Electronic Components and Technology Conference* pp. 1019.
- [9] G. Arlt, D. Hennings and G. de With. (1985, Dielectric properties of fine-grained barium titanate ceramics. *J. Appl. Phys.* pp. 1619.
- [10] T. Ohno, D. Suzuki and T. Ida. (2004, Size effect for barium titanate nano-particles. *KONA* 1(22), pp. 195.
- [11] K. Uchino, E. Sadanaga and T. Hirose, "Dependence of the Crystal Structure on Particle Size in Barium Titanate," *Journal American Ceramic Society*, vol. 72, pp. 1555, 1989.
- [12] K. Kinoshita and A. Yamaji. (1976, Grain-size effects on dielectric properties in barium titanate ceramics. *Journal of Applied Physics* 47(1), pp. 371.
- [13] M. Trainer, "Ferroelectrics and the Curie-Weiss Law," *European Journal of Physics*, vol. 21, pp. 459, 2000.

- [14] A. S. Shaikh, R. W. Vest and G. M. Vest. (1989, Dielectric properties of ultrafine grained BaTiO<sub>3</sub>. *IEEE Transactions on Ultrasonics, Ferroelectrics and Frequency Control* 36(4), pp. 407.
- [15] M. H. Frey, Z. Xu, P. Han and D. A. Payne. (1998, The role of interfaces on an apparent grain size effect on the dielectric properties for ferroelectric barium titanate ceramics. *Ferroelectrics* 206-207pp. 337.
- [16] D. Balaraman, P. Markondeya Raj, I. R. Abothu, S. Bhattacharya and S. Dalmia. (2003, Integration and high-frequency characterization of PWB-compatible pure barium titanate films synthesized by modified hydrothermal techniques. *IEEE Electronic Components and Technology Conference* pp. 1520.
- [17] M. P. McNeal, S. Jang and R. E. Newnham, "The effect of grain and particle size on the microwave properties of barium titanate," *Journal of Applied Physics*, vol. 83, pp. 3288, 1998.
- [18] Evans Analytical Group, "X-Ray Diffraction from Evans Analytical Group," vol. 2007, 2007.
- [19] J. Schlup. Conversation regarding X-ray diffraction.
- [20] W. F. Smith and J. Hashemi, *Foundations of Materials Science and Engineering*. ,4th ed. McGraw-Hill, 2005, pp. 1056.
- [21] Unknown, "Particle size and strain analysis by X-ray diffraction application note," H&M Analytical Services, 2002.
- [22] Evans Analytical Group, "Scanning Electron Microscopy (SEM) from Evans Analytical Group," vol. 2007, 2007.
- [23] W. Zhong, P. Zhang, Y. Wang and T. Ren, "Size Effect on the Dielectric Properties of BaTiO<sub>3</sub>," *Ferroelectrics*, vol. 160, pp. 55, 1994.
- [24] Kaiser Optical Systems Inc., "Raman Tutorial," vol. 2007,
- [25] I. Ueda, M. Takiuchi, S. Ikegami and H. Sato, "Dielectric Breakdown of POLycrystalline BaTiO<sub>3</sub>," *Journal Fo the Physical Societ of Japan*, vol. 19, pp. 1267, 1964.
- [26] Harpaintner, Alfons (Sr. Mgr. R&D Vishay). (2007, Personal communication regarding industry testing of dielectric material.